UNIVERSITAT POLITÈCNICA DE CATALUNYA
BARCELONATECH
Escola d'Enginyeria de Barcelona Est

BACHELOR'S THESIS

Chemical Engineering

SALINITY REMOVAL FROM PHREATIC WATER USING NANOFILTRATION MEMBRANES

Report and Annexes

Author: Josep Nadal Goday
Director: Oriol Gibert Agulló
Co-Director: Julio López Rodríguez

Convocation: January 2020

Resum

Aquest projecte tracta sobre la caracterització i dessalinització de l'aigua freàtica de la zona de Sant Adrià del Besòs, Catalunya, per a millorar-ne la qualitat i fer-la apta per a nous usos i en el millor dels casos adequar la seva composició a la d'aigua potable (RD 140/2003). La composició d'aquesta aigua varia segons l'època i les condicions de l'any, i, per a arribar a ser aigua potable, caldria eliminar els excessos de ferro, manganès, arsènic, amoni i clorur. Les plantes de tractament d'aquests tipus d'aigües requereixen una etapa per eliminar cada element no desitjat. Des de fa anys, la nanofiltració ha anat creixent com a mètode alternatiu a aquests tractaments, ja que permet l'eliminació d'aquests components mitjançant una sola etapa.

Inicialment, es va caracteritzar l'aigua i es va observar que contenia excessos de manganès, arsènic i clorur: 141,6 ppb, 126,0 ppb i 335,2 ppm, respectivament. Es van avaluar 3 membranes comercials fetes de poliamida com són la NF270, NF90 i DL en un mòdul de membrana pla (140 cm^2) d'escala laboratori. Es va estudiar l'efecte de la pressió trans-membrana, des de 6 bar fins a 32 bar per determinar les qualitats del permeat i si aquestes estaven d'acord amb els valor del RD 140/2003. Es van obtenir rebutjos elevats per als ions divalents i trivalents a concentracions de ppb (DL < 70%; NF90 < 80%; NF270 < 84%) i ppm (DL < 90%; NF90 < 99%; NF270 < 88%). Pel que fa al clorur i manganès, aquests van ser rebutjats fins a situar-se per sota dels límits dictats pel govern espanyol (RD 140/2003) amb les tres membranes; Els rebuigs obtinguts de clorur i manganès varen ser superiors al 55% i 89%, respectivament. En quant a l'arsènic, la membrana NF270 va rebutjar el 98% fent el seu permeat potable, mentre que les membranes NF90 i DL van obtenir rebutjos al voltant del 82%, que són resultats satisfactoris si es treballa amb aigües de menys de 52 ppb d'arsènic. A més a més, es va utilitzar el model de dissolució-difusió i pel·lícula (SDFM, per les seves sigles en anglès) per modelitzar el transport d'ions mitjançant les seves permeabilitats.

Resumen

Este proyecto trata sobre la caracterización i desalinización del agua freática de la zona de San Adrián del Besós, Cataluña, para mejorar su calidad i hacerla apta para nuevos usos i, en el mejor de los casos adecuar su composición a la de agua potable (RD 140/2003). La composición de esta agua varía según la época y las condiciones del año, y para conseguir el estatus de agua potable, se debería eliminar excesos de hierro, manganeso, arsénico, amonio y cloruro. Las plantas de tratamientos de este tipo de aguas requieren una etapa para eliminar cada elemento no deseado. Desde hace años, la nanofiltración ha ido creciendo como método alternativo a estos tratamientos, ya que permite la eliminación de estos componentes mediante una sola etapa.

Inicialmente, se caracterizó el agua i se observó que contenía excesos de manganeso, arsénico y cloruro: 141,6 ppb, 126,0 ppb i 335,2 ppm, respectivamente. Se evaluaron 3 membranas comerciales hechas de poliamida como son la NF270, NF90 i DL en un módulo de membrana plano (140 cm^2) a escala de laboratorio. Se estudió el efecto de la presión trans-membrana, desde 6 bar hasta 32 bar para determinar las calidades del permeado y si estas se ajustaban con los valores del RD 140/2003. Se obtuvieron rechazos elevados para los iones divalentes i trivalentes con concentraciones de ppb (DL < 70%; NF90 < 80%; NF270 < 84%) i ppm (DL < 90%; NF90 < 99%; NF270 < 88%). En cuanto al cloruro y manganeso, estos fueron rechazados hasta situarse por debajo de los límites dictados por el gobierno español (RD 140/2003) con las tres membranas; Los rechazos obtenidos de cloruro y manganeso fueron superiores al 55% y 89%, respectivamente. Con respecto al arsénico, la membrana NF270 rechazo el 98% obteniéndose así un permeado potable, mientras que las membranas NF90 y DL obtuvieron rechazos de alrededor del 82%, que son resultados satisfactorios si se trabaja con aguas de menos de 52 ppb de arsénico. Además, se utilizó el modelo disolución-difusión i película (SDFM, por sus siglas en inglés) para modelizar el transporte de iones mediante sus permeabilidades.

Abstract

The purpose of this project is the characterization and desalination of groundwater in the area of Sant Adrià del Besòs, Catalonia, in order to improve its quality and make it suitable for other uses and in the best of cases, upgrade its quality to the status of drinkable water (RD 140/2003). The composition of this water varies depending on the season and the meteorological conditions of the year. Excesses of iron, manganese, arsenic, ammonium and chloride need to be removed so that the condition of drinkability can be achieved. Treatment plants of this kind of waters normally require one stage for every substance that needs to be eliminated. For years, nanofiltration has grown as an alternative method to these treatments due to its capability of removal with only one stage.

Initially, the water was characterized and excesses of manganese, arsenic and chloride were observed: 141,6 ppb, 126,0 ppb I 335,2 ppm, respectively. Three commercial membranes made of polyamide were evaluated (NF270, NF90 and DL) in a flat membrane module (140 cm^2) at a laboratory scale. In order to determine the permeate quality and its compliance with the RD 140/2003, the effects of trans-membrane pressure were studied, from 6 bar to 32 bar. High rejections were obtained for divalent and trivalent ions at ppb (DL < 70%; NF90 < 80%; NF270 < 84%) and ppm concentrations (DL < 90%; NF90 < 99%; NF270 < 88%). Chloride and manganese were rejected to the point of compliance with the Spanish regulations of drinkable water RD 140/2003 using all three membranes; its rejections were higher than 55% and 89%, respectively. Regarding arsenic, the NF270 membrane removed 98% from the solution making it drinkable, while the NF90 and DL membranes removed around 82%. For these last two membranes, its results are satisfactory as long as the feed water contains arsenic lower than 52 ppb. Moreover, the solution-diffusion film model (SDFM) was used in order to represent the ion transport through its permeabilities.

Acknowledgements

First, I want to thank Julio López for his unconditional help and guidance. I really appreciate your patience at the laboratory and the support you provided me with. Without you the realization of this challenging project would have been extremely difficult.

I also want to thank Carme Gil Garcia for the emotional support and for cheering me up on my bad days.

Finally, I want to thank Jacqueline Perdula for being able to recharge my batteries and to keep me from giving up.

Glossary

BOE: “Boletín Oficial del Estado”

EDL: Electrical Double Layer

FS: Flat sheet

ICP-MS: Inductively coupling plasma mass spectrometry

IEP: Iso-electric point

J_v: Trans-membrane flux

MF: Microfiltration

MWCO: Molecular weight cut-off

NF: Nanofiltration

PACl: aluminium chlorhydrate coagulant

ppb: Parts per billion or µg/L

ppm: Parts per million or mg/L

ppt: Parts per trillion or ng/L

RO: Reverse osmosis

SCMZ: Silicate-Carbon Modified Zeolite

SDEFM: Solution-diffusion-electro-migration-film model

SDFM: Solution-diffusion film model

SDM: Solution-diffusion model

SW: Spiral wound

TMP: Trans-membrane pressure

TOC: Total organic carbon

UF: Ultrafiltration

WAC: Weak acid cation

Index

1. Introduction

1.1. Project Objectives

The objectives of this project are:

- To determine the water composition and compare it with the studies done in the previous years.

-To treat the water using nanofiltration (NF) membranes.

-To check if the composition of the permeate complies with the legal range for drinkable water.

- To compare the rejection behaviour of each membrane with its composition.

-To describe the ion transport using the solution-diffusion film model (SDFM)

1.2. Project Scope

The investigation and results of this project encompass only the underground waters of the Besòs area and the types of membranes used. The extrapolation of these results for any other project should be used only as a mere guideline.

2. State of the Art

2.1. Origin of the project

Sant Adrià del Besòs is a municipality located between Barcelona and Badalona, Spain. This zone is rich in groundwater, which once was over-exploited for industrial uses. At that time, constructions such as tunnels, underground parking places and basements were built. Due to the over-use of the phreatic water, the piezometric level stayed below the lowest level of those constructions, so no problem arose. Over time, the intensive usage of groundwater diminished due to the worsening of its quality. Because of this, the piezometric level arose, and underground structures started to be flooded. Constructions such as the underground parking lot of Sant Adrià del Besòs suffered from seepage and flooding and needed a pumping system to drain the water. The pumping system solved the critic situation by continuously extracting water at a flow of 250-300 $\frac{L}{s}$. Although the problem was temporarily solved, the situation was not sustainable due to high economic costs, therefore the city council decided to remodel the underground facility. Even after the remodelling, that turned a three-story into a two-story underground facility, a drainage system was still required. Nowadays, the system pumps roughly 150 $\frac{L}{s}$ of water that ends up in the sewers. A small portion of this water is used for gardening, but the most part of it is discarded. According to the water standards of the Spanish government RD 140/2003, this water does not comply with the quality limits of drinkable water due to their relatively high concentrations of ammonium, manganese, iron and arsenic (1).

The origin of this project came along with the idea of using this pumped water for other purposes other than just throwing it away. The goal then is to investigate if this water could be used for domestic and industrial purposes. In order to achieve this goal, a treatment is researched. The water treatment that will be applied and explained in this thesis is to be done using membrane technology, specifically Nanofiltration (NF).

2.2. Importance of the project

Water is one of our most valuable resources, and it is not unlimited. Every possible source of extraction should be considered and studied. All the drained water from the parking lot of Sant Adrià del Besòs is now pumped away into the sewers. This current situation is one of misuse. That water could satisfy part of the demand of the city and could also help in other extreme situation like droughts.

Regions like Catalonia, Spain, have already suffered from heavy droughts in the past such as the one that happened in 2008. At the beginning of the year water needed to be brought to Barcelona by boat

from Tarragona and France. Catalonia cannot always rely on these last minute solutions and needs to be prepared.

Those situations of emergency could be relieved if auxiliary systems of water purification and extraction were available like the case with phreatic water from Sant Adrià del Besòs.

There are various methods of water purification used nowadays. One of the most known ones is the Reverse Osmosis (RO). It has been proved to be effective in the desalination and recovery of water for drinkable purposes. Although it is effective, it comes with a high cost of energy due to the high pressure difference that needs to be applied (2).

The importance of this project lies in the use of cheaper technology, such as nanofiltration, to see if water desalination and metallic ion removal can be achieved with efficiency. NF is less expensive because it needs lower pressure difference, such as 2 bar, were substantial ion removals are stated in the study carried out by Pages, N. et. al (3).

2.3. Technologies used nowadays

A previous study has been made about the underground water compositions of the Besòs area before the beginning of this project. Six field campaigns were carried out starting July 2007 and finishing July 2014 (July 2007, February 2008, October 2008, May 2010, December 2013 and July 2014) (1).

The average concentrations of each campaign (from C1 to C6) are summarized in Table 1 and Table 2. When speaking of phreatic water, it needs to be taken into account that its composition is closely dependent on the water inflows that recharge them, e.g. rivers, lakes, glaciers, etc. Therefore, changes in the underground water composition may arise due to variations of the state of the inflows or seasonal changes. Due to the severe drought that happened in Catalonia in 2007-2008 the sampling campaigns carried out in that period (C1-C3) showed higher mineral concentration than in the later ones (C4-C6) where rains caused the dilution effect. This fact was reflected in the concentrations of bicarbonate, sodium, potassium, calcium, chloride, sulphate, magnesium, and ammonium. Concerning metals concentrations, the highest concentrations were also found in the first campaigns especially in C1 and C2 (1).

Table 1. Concentration ranges and average concentrations (in parentheses) of major ions, ammonium, dissolved oxygen and total organic carbon for each sampling campaign (C1–C6) in mg/L, and electrical conductivity (µS/cm) (1).

Chemical parameter	Sampling campaign						Cm	RD 140/2003
	C1	C2	C3	C4	C5	C6		
Chloride	241.5–308.3 (268.1)	242.3–297.6 (268.8)	249.7–278 (259.7)	181.7–211.8 (199.5)	171.9–221 (191.8)	178.9–213.4 (192.9)	229	250
Sulphate	151.7–172 (164.4)	177.3–181.4 (179.3)	155.3–166.5 (160.7)	139.1–165.1 (150.3)	135.2–158.8 (146.8)	122.7–142.1 (135)	155.8	250
Bicarbonate	401–455.9 (428.1)	425.4–470.5 (449)	403.5–442.5 (426.6)	391.3–433.9 (412)	397.8–418.1 (406)	367–410 (399.6)	419.1	–
Calcium	131.4–146.8 (138.6)	137.5–149 (142.7)	129.4–147.9 (138.7)	117.3–135.4 (128.2)	106.4–120.7 (114.6)	92.3–120.9 (111.4)	128.7	–
Magnesium	28.2–29.6 (28.8)	23.6–33 (29.4)	28.1–31.9 (29.6)	25.2–28.7 (27.3)	21.2–25.3 (23.5)	19.8–25.4 (23.1)	26.9	–
Sodium	204–257.3 (225.6)	188.2–211.4 (200)	197.4–224 (209.1)	146.3–165.4 (146.3)	119.5–153.4 (137.3)	120.5–157 (133.8)	175.6	200
Potassium	16.3–28.1 (21.6)	18.2–21.2 (20.1)	16.4–24 (20.8)	14.9–21.3 (17.6)	10.5–15.7 (13.4)	11–21.2 (14.5)	17.9	–
Nitrate	0–14.3 (2.9)	0–24.7 (4.3)	<LOQ–10.1 (2.3)	0–3.7 (0.8)	0–12.4 (5.9)	0–13.2 (7.3)	3.9	50
Ammonium	2–15.2 (8)	4.7–11.8 (7.7)	4–9 (6.5)	2.1–6.3 (4)	1.2–5.8 (2.7)	0.6–6.6 (2.2)	5.1	0.5
Electrical conductivity	1,501–1,780 (1,631.2)	1,581–1,757 (1,654.8)	1,552–1,646 (1,595.8)	1,277–1,438 (1,375.5)	1,293–1,460 (1,360.2)	1,389–1,574 (1,444.3)	1,506.9	2,500
Total organic carbon	2.6–6.1 (3.9)	3–6.6 (4.3)	2.2–4.7 (3.4)	2.5–4.5 (3.3)	1.5–3.4 (2.3)	1.5–5.2 (2.9)	3.3	–
Dissolved oxygen	0.03–0.24 (0.01)	0.04–1.1 (0.4)	0.1–0.2 (0.1)	0.65–2.3 (1.2)	0.1–1.4 (0.3)	0.15–0.19 (0.2)	0.4	–

Note that *Cm* is the average concentration considering all of the sampling campaigns. *RD 140/2003* represents the recommended limits for Spanish drinking water guidelines. *LOQ* limit of quantification

Table 2. Concentration ranges and average concentrations (in parentheses) of metals for each sampling campaign (C1–C6) in µg/L (1).

Metal	Sampling campaign						Cm	RD 140/2003
	C1	C2	C3	C4	C5	C6		
Aluminium	7.1–287.6 (93)	0.9–601.3 (161.6)	0–59.26 (17.6)	0–≤LOQ	5.5–23.5 (13.8)	9.5–67.1 (38.4)	53	200
Arsenic	2.4–31.1 (14.8)	4–27.5 (17.1)	3.6–32.2 (16.6)	2.1–17.3 (10.8)	1.6–9.1 (5)	1.5–14.5 (6.4)	11.7	10
Boron	260.7–283.3 (270.2)	229.2–298.9 (266.8)	199.3–264.9 (231.4)	138.2–201.7 (177.6)	163.4–244.3 (207.9)	171.6–223.5 (202.4)	224.8	1,000
Cadmium	<LOQ	<LOQ	0	0	<LOQ	<LOQ	0.4	5
Chromium	7.2–12.8 (9.6)	10.3–17.4 (14.3)	9.9–13.2 (11.2)	1.7–18.5 (12.8)	<LOQ–2.9 (2.3)	<LOQ–2 (1.5)	8.6	50
Copper	1.7–5.4 (3.6)	1.6–12.7 (6.3)	1.3–6.4 (3.4)	1.4–13.7 (5.8)	1–2.8 (2.1)	<LOQ–2.5 (2)	3.9	2,000
Iron	128.2–1563.5 (589.7)	59.9–3595.3 (891.2)	65.4–1610.5 (509)	19.6–554.7 (203.6)	12–536 (185.5)	19.9–414.7 (187.2)	423.1	200
Manganese	175.7–406.6 (285.2)	186.3–588.6 (319.2)	192.5–824.3 (388.4)	64.1–810 (292.6)	2.3–433.2 (133.6)	1.9–382.9 (133.9)	258	50
Nickel	5.2–8.4 (6.5)	6–8.3 (7)	3.4–5 (4.2)	4–6.5 (5.7)	2.2–3 (2.6)	3.8–4.3 (4)	5	20
Lead	<LOQ–1.7 (1.2)	0.81–7.1 (3.4)	<LOQ–1.1 (0.68)	<LOQ–1 (0.32)	<LOQ	<LOQ–1.5 (0.58)	1.1	10

Note that *Cm* is the average concentration considering all of the sampling campaigns. *RD 140/2003* represents the recommended limits for Spanish drinking water guidelines. *LOQ* limit of quantification

A great array of technological options is available for water treatment. Each choice depends on the conditions and quality of the water. As can be seen, the phreatic water from Sant Adrià del Besòs presents higher concentrations of manganese, iron, ammonium and iron than the values established by the recommended limits for the Spanish water guidelines (RD 140/2003). In the next sections the techniques used for the removal of those elements will be discussed.

2.3.1. Manganese

Manganese is a transition metal that can lead to neurodegenerative disorders, if excessive exposure or intake happens, e.g. very high levels of manganese dusts or fumes (4). Even though, problems due to manganese intake by drinking water are not possible when the Spanish drinking water guidelines are met. The following technics are used for the removal of manganese:

- One of the most common methods for the removal of manganese is oxidation by aeration or by using strong oxidizing agents such as potassium permanganate and then removal by filtration. The percentage removal varies depending on the conditions of the oxidation. The most successful ones range from 87% to 99 % (5). In acid or neutral solutions the ion Mn^{2+}exists as $[Mn(H_2O)_6]^{2+}$ which resists oxidation. However, if the medium becomes basic the following reactions occurs: (6)

$$[Mn(H_2O)_6]^{2+}(aq) \xrightarrow[pH[9-10]]{} Mn(OH)_2(aq)$$

$$Mn(OH)_2(aq) \xrightarrow[Oxidation]{} \mathrm{MnO_2}(s) \downarrow$$

- Adsorption is another method for the removal of manganese from water. The use of adsorbents like Zeolites or modified Zeolite with NaOH 1,5 M solutions (for an improvement of the adsorption capacity) are proved to work in waters with Mn^{2+}ranging from 25 to 250 ppm (7).

2.3.2. Iron

Iron is not considered to be a health hazard as long as it does not surpass the drinkable limit ranging from 0,2 to 0,3 ppm (depending on the country). However, its presence in water is rather unpleasant due to its rusty taste, odour, colour and tendency to stain clothing (8).

In surface waters, dissolved iron is hardly ever found due to the presence of oxygen. Iron is oxidized and then forms insoluble compounds that precipitate. Conversely, iron is one of the most common dissolved chemicals found in underground waters since oxygen exists in far lower concentrations than on the surface. The following technics are used nowadays for the removal of iron in water:

- Oxidation-Filtration: In this case iron is oxidized, precipitated (pH 8,5-9,5 (9)) and then removed. Normally for the oxidation chlorine dioxide (ClO_2), ozone (O_3) or potassium permanganate ($KMnO_4$) are used. Moreover, an aeration technique can be used for a more environmentally friendly option (8).

$$Fe^{2+}(\text{aq}) \xrightarrow[Oxidation]{} Fe^{3+}(\text{aq}) \xrightarrow[Precipitation]{} \text{Fe}(OH)_3(s) \downarrow$$

- Coagulation-Flocculation: This method is rather used for the removal of high quantities of suspended solids in the water. Coagulants neutralize the repulsive charges of the colloids and flocculants conglomerate those destabilized particles to precipitation. Pong et al. (10) removed iron from a solution containing 7 ppm Pb (II) with Fe (III) concentration varying from 5 to 45 ppm using the following coagulants: alum ($Al_2(SO_4)_3$), PACl (aluminium chlorhydrate) and $MgCl_2$. The resultant effluent contained a concentration lower than 0,2 ppm Fe (III).

2.3.3. Ammonium

Water ammonium contamination can happen in acid mine drainage and in waters located near agriculture fields due to the use of fertilizers which usually contain high amount of ammonium. The following methods can be used for the removal of ammonium in water:

- Adsorption: Li et al. (11) used Silicate-Carbon Modified Zeolite (SCMZ) for ammonium removal from drinking water. The results showed that the adsorption capacity of SCMZ was 0,115 mg $NH_4^+ - N$/g, when the pH of the solution was 7 and initial ammonium concentration was 5 ppm. Ammonium removal efficiency of the SCMZ and natural zeolite varies with the filtration rate, regeneration cycles of the zeolite and initial ammonium concentration.
- Ion exchange: Malovanyy et al. (12) removed and concentrated ammonium using glass packed bed columns filled with four different ion exchange materials: Zeolite rock containing 70–75% clinoptilolite, Synthetic zeolite of NaA type, SAC resin KU-2-8 (sulfonated polystyrene type, divinilbenzene content) and WAC resin Purolite C104 (carboxylic functional groups). Ammonium removal efficiency ranged from 88% to 99,9% depending on the material used.

2.3.4. Arsenic

Arsenic is a toxic metalloid element. According to the World Health Organization the maximum level of Arsenic in drinkable water is of 10 μg/L. In order to avoid higher concentrations in drinkable water, the following techniques are used:

- Coagulation–precipitation: Chemicals are used to transform dissolved arsenic and co-precipitate it with the added chemicals. Commonly used chemicals in this technique are ferric salts, alum, manganese sulphate, ammonium sulphate, copper sulphate, etc. (13). Using $FeCl_3$ or alum independently at a neutral pH As (V) removal efficiency was higher than 90% for a feed concentration of 20 ppb (14).
- Lime softening: This technique is similar to precipitation where limes (limestone, calcium hydroxide) are the medium used for the removal that. At pH ≥ 10,5 the performance of removal ranges from 80% to 90% for a feed concentration of less than 50 ppb (13).
- Adsorption: In this process arsenic species within the solvent become attached to the surface of the adsorbent. Conventionally used adsorbents are activated alumina, activated carbon, greensand ($KMnO_4$ coated gluconite), granular ferric hydroxide, iron oxide coated sand, copper-zinc granules, etc. The yield of these arsenic removal processes depends on the conditions and the absorbents, it can range from 23% to 96% (14)(15).
- Ion exchange: An anion exchange resin captures the arsenic anions and at the same time releases similar charge non-toxic ions into the solution (13). A study was made concerning the removal of arsenate and nitrate from water using anion exchange. The results showed that separation was possible as long as the raw waters did not contain substantial concentrations of sulfate (200ppm). In that case the resin would become exhausted quickly making the process unattractive (16).
- Electro dialysis: An electric field acts as driving force across a semi permeable ionic exchange membrane making the separation possible (13).

As listed before, there are lots of separation techniques and procedures to choose from for the removal of the elements of interest (see Table 3). In order to achieve that goal, a combination of physical and chemical separation stages is normally needed. Instead, the possibility of a one stage procedure is discussed. The one elected to be the subject of this Bachelor Thesis is pressure-driven membrane filtration, which provides the simplicity of a one stage process and the non-use of chemicals.

Table 3. Summary of the different technics applied to the removal of each ion.

Technics	Manganese	Iron	Arsenic	Ammonium
Oxidation/Precipitation	X	X	X	
Adsorption	X		X	X
Ion exchange			X	X
Electro dialysis			X	
Lime softening			X	
Coagulation/ precipitation		X	X	

It should be keep in mind that there might exist more treatments for the removal of the elements showed in Table 3. The table should be seen as a mere guideline.

2.4. Membrane technology

A membrane is a thin, permeo-selective barrier that separates two phases from each other and opposes the transport of chemical components according to their selectivity (17). The membrane filtration techniques discussed in the following lines use a pressure difference as a driving force for the separation. The removal efficiency of organic and ionic species depends on the pore size of the membrane and the particle size of the species to be separated as well as the pressure difference applied and other environmental factors such as acidity (18). Furthermore, for the removal of ionic species the charge and the electric effects (which are explained in 2.6) also play a significant role.

When speaking of filtration membranes, it is important to point out that there are different kinds of them. On one hand, there are the porous membranes, and on the other hand, there are the dense membranes. Microfiltration (MF) and ultrafiltration (UF) are the porous ones whereas NF and RO are the dense ones. Dense membranes do not have fixed pores. Instead they have free volume that comes from the movement of the polymeric chains that forms the membrane. The bigger the pore or free volume, the more species will get through the membrane into the permeate (18). The illustration below (Figure 1) shows each membrane type with its pore or free volume size as well as the species that rejects.

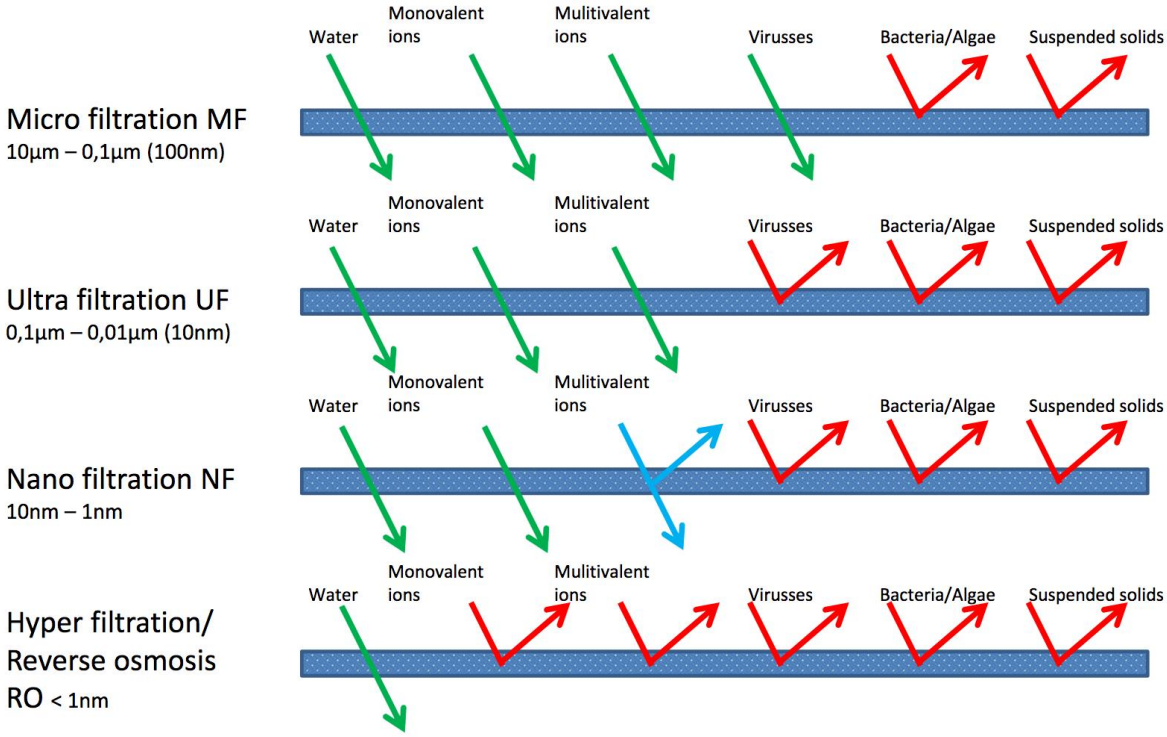

Figure 1. Comparison Membrane Techniques (19)

Similar to RO membranes, NF membranes are powerful separating inorganic salts and small organic molecules. NF membranes have low rejection of monovalent ions and high rejection of divalent ones. Despite the fact that RO membranes have higher ion rejections, NF have higher transmembrane flow (20). Moreover, NF membrane offer other advantages such as lower operational pressure, lower investment, operation and maintenance costs (21).

2.4.1. Nanofiltration

NF membranes are used in many applications especially in water, wastewater and desalination. RO and NF membrane types share the same workings schematics. These are illustrated in the Figure 2. As it can be seen, there is one input and two output flows. The feed represents the solution that needs to be treated. The fraction of it that permeates through the membrane is called permeate, and it presents a lower content of solutes than feed due to their retention by the membrane. The fraction that does not permeate through the membrane is called concentrate, and it presents higher content of solutes than feed as it contains the solutes rejected by the membrane (17).

By and large, when speaking of water treatment, the permeate is the outcome flow of interest because is free of undesired components and can be eventually used as drinking water or any other use.

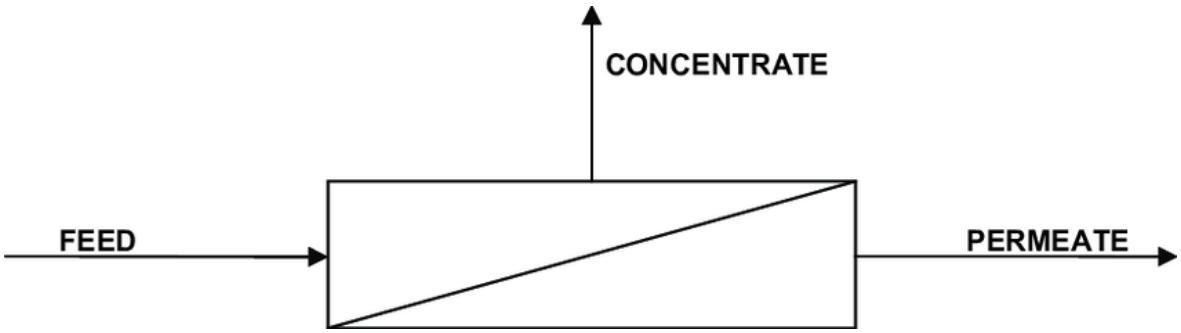

Figure 2. Separation schematics of a membrane filtration system

The membrane ability to separate species is represented by the rejection (Eq. 1) stated bellow.

$$R = \frac{c_F - c_P}{c_F} \qquad \text{Eq. 1}$$

Where:

- R = Rejection $[\%]$
- c_F= Feed concentration of the species $[ppm]$
- c_P= Permeate concentration of the species $[ppm]$

Generally for NF membranes divalent and trivalent ions are rejected with values of around 99%. Rejections of monovalent ions are much lower, between 20% and 70%, and are more dependent on the conditions of the solution to be treated and the composition of the membrane. This property is an intermediate between RO membranes with a salt rejection of more than 95% and UF membranes with a salt rejection of less than 10% (21).

Changes in the trans-membrane pressure (TMP) affect the trans-membrane flux (J_V) (As rule of thumb the higher the pressure the higher the flux) which also affect the rejection. With a controlled variation of the J_V, rejection curves can be drawn as it appears in Figure 3.

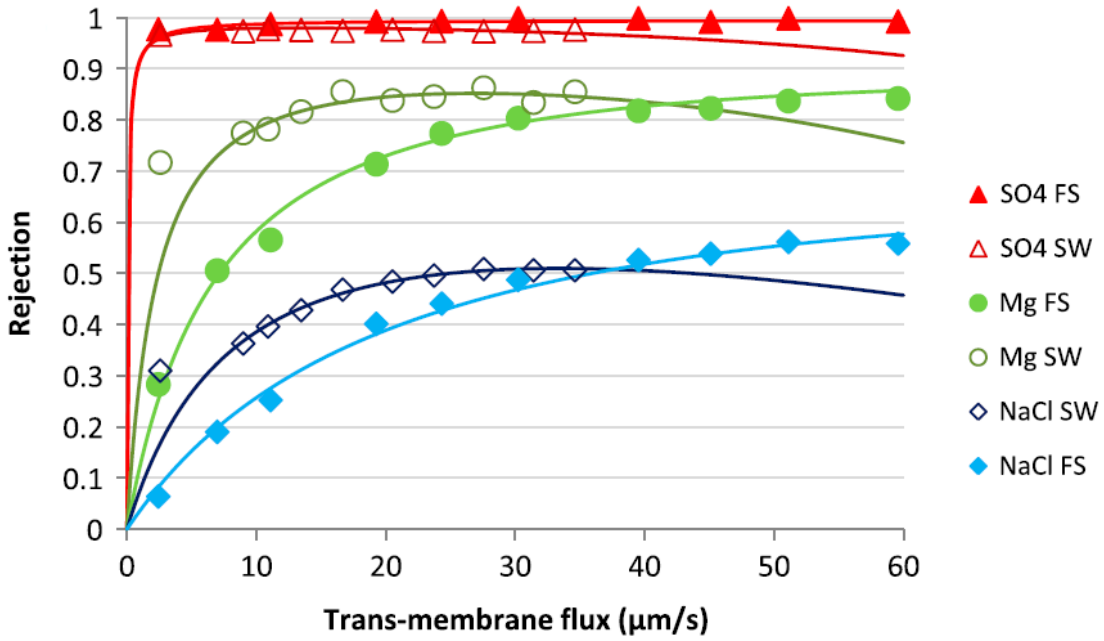

Figure 3. Comparison between rejections experimentally obtained and rejections predicted with the solution-diffusion-electro-migration-film model (SDEFM) using a flat sheet (FS) and a spiral wound (SW) membrane configuration using NaCl as dominant salt and $MgSO_4$ as trace (21).

When working with membranes, it is important to take the fouling into account. Membrane fouling occurs when elements, such as colloids and organic or inorganic particles, are deposited on the surface of the membrane. This restricts the flow through the pores of the membrane drastically reducing its efficiency (17).

NF membranes have an interesting factor that influences in a great deal the ion rejection, they present functional groups (e.g. polyamide-based membranes has amine and carboxylic groups) that get ionized in aqueous media. This confers the membrane a superficial charge that will be positive or negative depending on the pH of the solution. The iso-electric point (IEP) is defined as the pH value where the membrane has no charge. This allows the arising of spontaneous electric fields in the membrane phase. For example, at pH<IEP, the amine and carboxylic groups of a polyamide membrane are partial and fully protonated (i.e. $R\text{-}NH_3^+$ / R-COOH), giving the membrane a positive surface charge. Then, cations will be rejected while the anions will be attracted to the membrane. Contrarily, at pH>IEP the membrane will present a negative charge due to the deprotonation of amine and carboxylic groups ($R\text{-}NH_2$ / $R\text{-}COO^-$). This negative charge will favour the transport of cations while the ones for anions is impeded (18).

As far as membrane operation is concerned, there are two different configurations: spiral wound (SW) and flat-sheet (FS). FS configuration are more used at laboratory scale due to its simplicity and reproducibility, although some FS modules at industrial scale can also be found. As its name indicates, FS membranes consist of a flat sheet that separates the different phases. In this configuration, the feed

solution is pumped into the module and then flows tangentially across the surface of the membrane surface. The applied pressure makes part of it to permeate (the filtration occurs in the perpendicular direction of the feed stream) and afterwards, this stream is collected as the permeate solution (Figure 4). On the other hand, SW configurations are implemented at industrial scale levels due to their higher specific surface area. SW modules are essentially, two or more membrane pockets wounded around a centrally located tube that collects the permeate. The membrane pocket consists of two membrane sheets with a fine plastic mesh properly designed in between, which are glued together along three edges, being the fourth edge of the pocket connected to the collecting tube. Here, the feed flows axially, while the permeate flows through the porous support inside the pocket and along the spiral pathway to the collecting tube (Figure 5) (21).

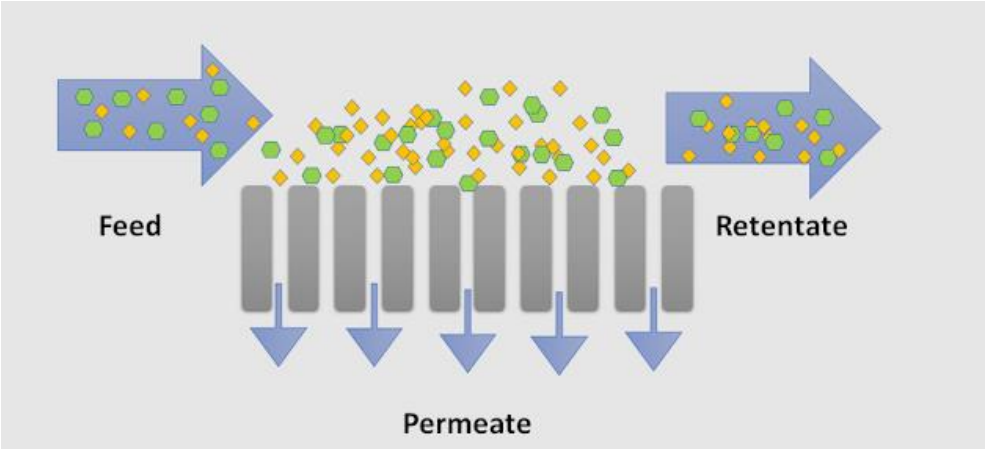

Figure 4. Cross-flow filtration mode (22).

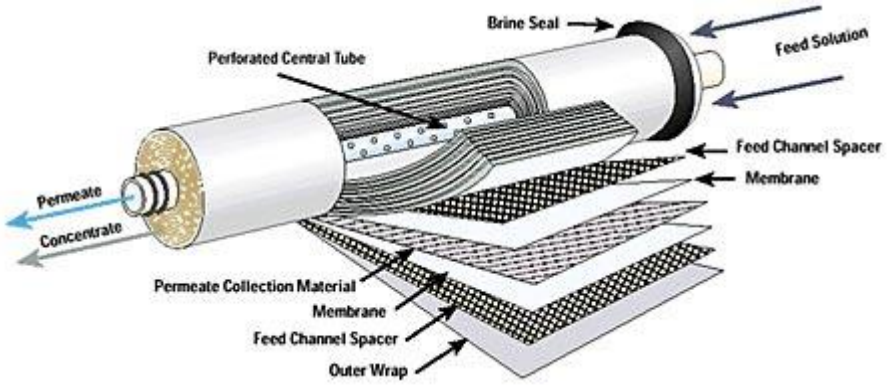

Figure 5. SW configuration (23).

In general, ion rejection curves for both configurations happen to be quite similar (21). Ribera et al. (24) concludes that experimentation at laboratory scale plant can be useful to design a full scale plant.

2.5. Membrane Transport Mechanisms

In order to foresee the flows and rejections of a NF membrane in a specific environment the transport mechanisms that take place need to be understood. These mechanisms depend on the propriety that dictates which species will pass through the membrane and which ones not: the permeability.

There are two models used to describe the substance transport: the pore-flow model and the solution-diffusion model.

2.5.1. Pore-flow model

This model is based on separation by size (Figure 6). The concept is simple, due to a pressure-driven convective force, the species of the feed solution are transported to the membrane where they encounter tiny pores. The species that are smaller than the pores will get through the membrane whereas the species that are bigger will not (18).

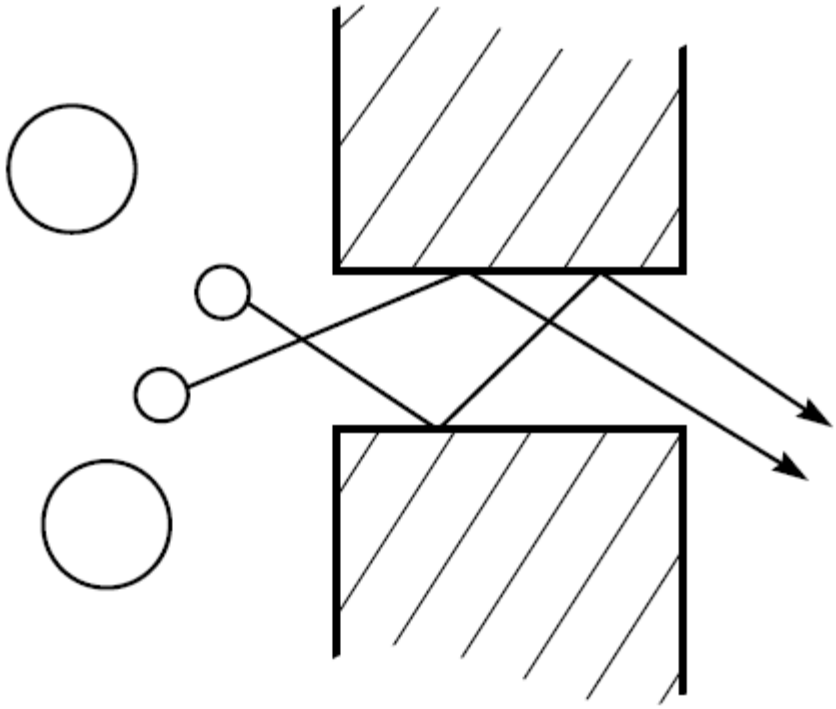

Figure 6.Pore-flow model: Microporous membranes separation by molecular filtration (18)

The basic equation covering this type of transport is Darcy's law, which can be written as (18):

$$J_i = K' c_i \frac{d_p}{d_x} \qquad \text{Eq. 2}$$

Where:

- J_i = Flux of the component "i" $\left[\frac{g}{cm^2 \cdot s}\right]$.
- K'= coefficient that reflects the nature of the medium $\left[\frac{cm^2}{bar \cdot s}\right]$.
- c_i = pressure gradient existing in the porous medium $\left[\frac{g}{cm^3}\right]$.
- $\frac{d_p}{d_x}$ = pressure gradient existing in the porous medium $\left[\frac{bar}{cm}\right]$.

2.5.2. Solution-diffusion model

The following model represents the solute separation through diffusion. When a concentration gradient occurs, permeants dissolve in the membrane, and then they diffuse through it. The separation occurs because of the differences in the solubilities of the solutes in the material of the membrane and the differences in the rates at which the solutes diffuse through the membrane (Figure 7) (18).

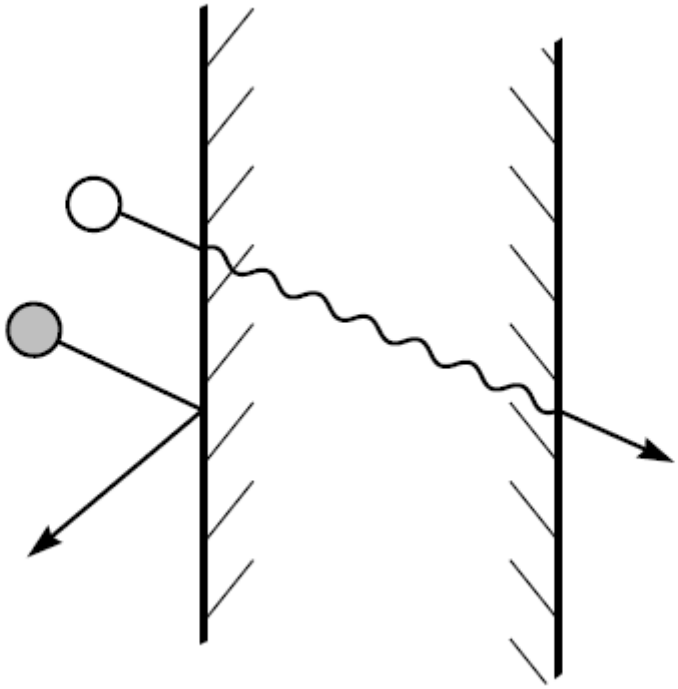

Figure 7. Solution-diffusion model: Dense solution-diffusion membranes separation due to differences in the solubility and mobility of permeants in the membrane material (18).

This concept was first recognized by Fick theoretically and experimentally in 1855 and then expressed with the following equation: (18)

$$J_i = -D_i \frac{d_c}{d_x} \qquad \text{Eq. 3}$$

Where:

- J_i = Flux of the component "i" $\left[\frac{g}{cm^2 \cdot s}\right]$.
- D_i = Diffusion coefficient $\left[\frac{cm^2}{s}\right]$.
- $\frac{d_c}{d_x}$ = concentration gradient of component "i" $\left[\frac{g}{cm^4}\right]$.

2.6. Transport phenomena

Different transport phenomena should be taken into account when filtering solutions with NF: the Donnan exclusion, the dielectric exclusion, the double electric layer and the concentration polarization.

2.6.1. Donnan exclusion

As mentioned before in section 2.4.1, when NF membranes are put in contact with a solution, their functional groups get ionized and then, the membrane exhibits a superficial charge. The Donnan exclusion is a phenomenon that happens when an electrostatic interaction occurs between the charged surface of the membrane and the ions of the solution (25).

There are two types of ions regarding to the membrane charge. The ions with the same charge sign as that of the membrane are the co-ions, the other with the opposite charge are the counter-ions. On one hand, the co-ions are excluded and cannot go through the membrane. On the other hand, the counter-ions are able to permeate (Figure 8). Nevertheless the electro neutrality of the solution must be maintained that is why enough co-ions (the most prone to permeate) will get through the membrane to keep it (21)(26).

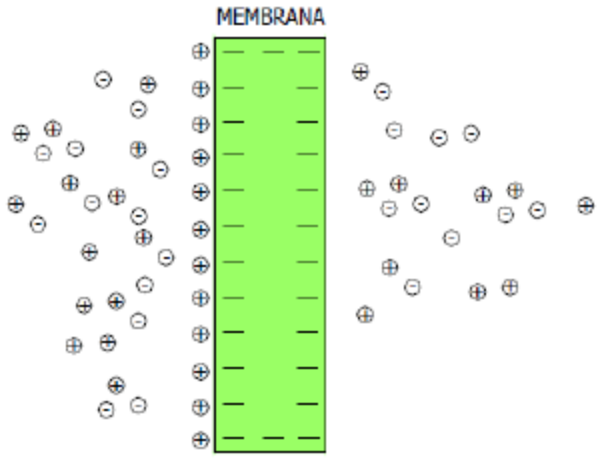

Figure 8. Donnan Exclusion Principle (27)

2.6.2. Dielectric exclusion

Dielectric exclusion is a phenomenon that happens whenever two or more media with different dielectric properties are put in contact. When speaking of NF membranes, these media are the aqueous solution and the polymeric matrix. Since the dielectric constant of the aqueous solution is significantly higher than the one of the membrane, electrostatic interactions arise between the ions of the solution and the polarized charges, induced by the ions themselves on the surface located where both media meet. The dielectric exclusion effect is therefore considered as an additional rejection mechanism caused by this difference existing between the dielectric constant of both media (28). The phenomenon is illustrated in Figure 9.

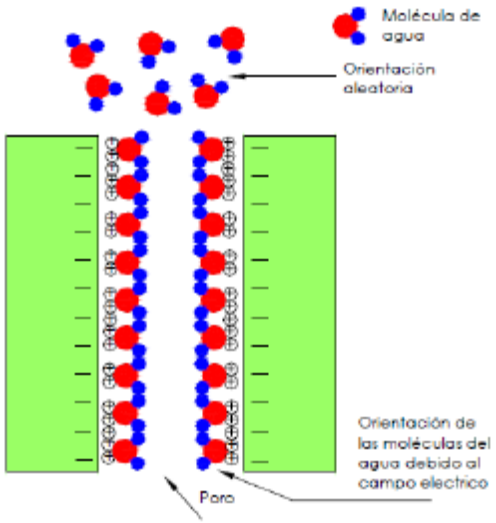

Figure 9. Representation of the dielectric exclusion (27)

2.6.3. Electrical double layer

The effect of the Electrical Double Layer (EDL) happens when a charged solid surface, like the membrane, attracts the counter-ions of the solution in order to maintain electro neutrality. The counter-ions spread themselves along the surface of the membrane generating a layer. This counter-ion coating is called the Debye length and its thickness is inversely proportional to the ionic strength of the solution in contact with the membrane. The thicker the layer the less ions will pass (both co-ions and counter-ions) and the other way around, the slimmer the coating the more ions will get through. The following image illustrates this phenomenon (29).

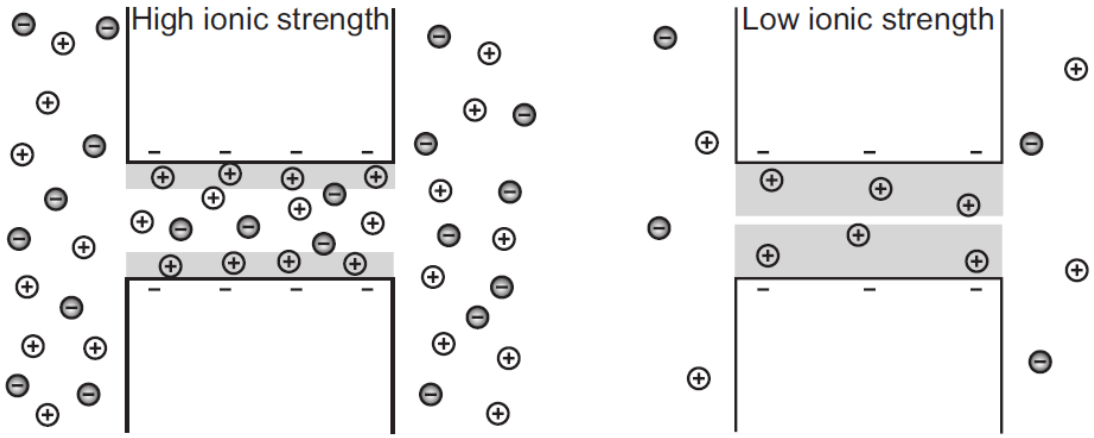

Figure 10.Electrical double layer EDL, shaded in grey at high ionic strength, it is thin, allowing co-ions and counter-ions to pass through the nano pores. At low ionic strength, the EDL thickness increases, resulting in a counter-ion-selective nano pore (29).

2.6.4. Concentration polarization

The concentration polarization phenomenon happens because the rejected solute accumulates on the surface of the membrane. Due to this, the interface membrane-solution happens to have a higher solute concentration than the solution itself. Consequently, a concentration profile occurs between the membrane surface and the solution. This profile is called the concentration-polarization layer (Figure 11) (30).

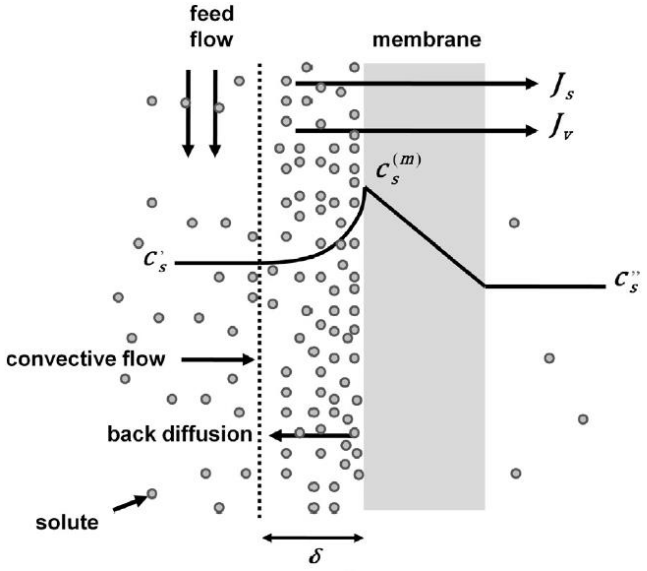

Figure 11. Schematic description of ion transport processes through both concentration-polarization and membrane layers (3).

2.7. Nanofiltration applications

The following lines are to give a brief idea of the projects and achievements of the NF technology regarding water treatments similar to those of this project:

- NF270 membrane rejected almost 100% of copper (feed concentration of 1000 ppm) within a brand range of pressures (3–5 bar) and pH (1.50–5) which demonstrates the suitability of NF270 for copper rejection. At pH=1.50 and 4 bar pressure, NF270 also removed about 99%, 89% and 74% of cadmium, manganese and lead, respectively. However, this membrane failed to reject As(III) as it obtained rejection values ranging from 0 to 11%. For copper, cadmium and lead, at higher concentrations (2000 mg/L) the rejection decreased to values of 58 ± 5% (31).
- Acid mine drainage was treated with RO and NF membranes (SW30 HR, Espa2, TFC ULP, RO1) in order to obtain clean permeate and a concentrate suitable for downstream treatment in nitrifying-denitrifying bioreactors. These waters contained 9.5 ppm of ammonium and 15.5 ppm of nitrate. RO yielded good quality permeate and concentrate for bioreactor treatment (retention of >97.4% for NO_3-N and >94.3% for NH_4-N,). NF showed poor separation performance (retention of 56.2%). A clear absence of dominant salt could have affected NF performance making its rejection lower and this way not suited as pre-treatment (32).
- Removal of iron and manganese from water with a high organic carbon loading using adsorbent and three NF membranes: NF70, NF90 and D11. The Table 4 shows the contaminant concentration after and prior treatment having used or not using adsorbents. Concerning Fe (II) all filter types, but the NF70 and D11 without treatment, achieved a drinkable permeate

according RD 140/2003 of the Spanish regulation. Concerning Mn (II), only the NF 70 with a H_2O_2 treatment achieved it (33).

		Feed concentration of contaminants (mg/L)			Permeate concentration of contaminants (mg/L)		
Filter type	Treatment	Fe(II)	Mn(II)	DOC	Fe(II)	Mn(II)	DOC
NF 70	None	2.96	0.29	8.3	0.21	0.10	2.4
	$FeCl_3$	3.22	0.24	6.6	0.14	0.08	1.4
	H_2O_2	2.71	0.15	6.4	0.07	0.05	2.2
	$FeCl_3$ and H_2O_2	3.52	0.17	5.6	0.13	0.12	3.9
NF 90	None	2.96	0.29	8.3	0.11	0.14	2.3
	$FeCl_3$	3.22	0.24	6.6	0.11	0.09	4.1
	H_2O_2	2.71	0.15	6.4	0.18	0.10	2.0
	$FeCl_3$ and H_2O_2	3.52	0.17	5.6	0.17	0.09	4.0
D 11	None	2.96	0.29	8.3	0.21	0.10	2.4
	$FeCl_3$	3.22	0.24	6.6	0.10	0.07	1.6
	H_2O_2	2.71	0.15	6.4	0.18	0.13	6.3
	$FeCl_3$ and H_2O_2	3.52	0.17	5.6	0.14	0.12	5.0

Table 4. Contaminant concentration before and after treatment

- Waters with total arsenic (5–50 mg/L) and As (III) (1–10 mg/L) were treated using three NF membranes: ES-10, NTR-729HF and NTR-725. For all NF membranes investigated, in pressure range of 0.3–1.1 MPa, As (V) rejection exceeded 85%, while As(III) proved to be far more difficult to remove, being the rejections lower than 22% using NTR-729HF and NTR-725, and higher than 75% using ES-10. Pre-oxidation treatment of As(III) may be needed for a higher removal of this element (34).
- Selective separation of chloride and sulfate was achieved using a NF membrane (Desal-DL) from high salinity waters. Different experiments were done by changing the concentrations of NaCl and Na_2SO_4 from 4 to 96 g/L. A lab scale cross-flow batch module was used where the operating pressures varied from 0,6 to 2,4 MPa. Finally, the selective separation was simulated for a feed solution containing 23,4 g/L of NaCl and 8,76 g/L of Na_2SO_4. A highly concentrated solution of Na_2SO_4 (71,74 g/L) and a relatively pure solution of NaCl (20,79 g/L) were obtained. This method can be used as pre-treatment for salt recycling from high saline wastewater (35).

3. Solution-Diffusion-Film Model

The solution-diffusion-film model (SDFM) can be used to describe the ion rejection of different single salts within the trans-membrane flux. It includes the ions from the dominant salt, which are those present in the solution at the highest concentration, and also the trace ions, which are ions in smaller amounts. This model takes into account that the transport of solutes occurs via diffusion and electric migration through the membrane as well as via convection in the concentration-polarization layer (Figure 11) (3). As stated in 2.4.1, the membrane ability to separate species is represented by its rejection. There are two different kinds of rejections: observable and intrinsic; the only difference between them is the concentration of origin chosen for its calculation. When the feed concentration is used the result is the observable rejection and when the concentration of the concentration-polarization layer is used the result is the intrinsic rejection. Therefore, the intrinsic rejection determines the ion removal from the membrane surface, whereas the observable rejection from the feed solution. Due to the concentration-polarization layer having a higher solute concentration than the feed solution, the observable rejection is always lower than the intrinsic rejection. It must be noted that there are concentration gradients of dominant salt within the concentration-polarization layer. As a result of the difference in the diffusion coeficients of these ions electric fields of diffusion origen are generated. These fields act on trace ions (3).

The solution-diffusion model (SDM) postulates that the transport is due to a combination of concentracion and electrostatic potential gradient and it assumes that there is no convective coupling between the water and the solute transfers (both solute and water are transported independently). This description of the trans-membrane solute transfer allows the development of efficient procedures to obtain the properties of membrane transport from experimental data. This is the case of the SDFM model because it can be used to find analytical solutions for the intrinsic rejection of traces versus the tans-membrane flux (J_v) $[m \cdot s^{-1}]$ from experimental data from both dominant and trace ions (3).

The protocol of data treatment for the SDFM model consists on the following:

1. From the experimental data, the values of J_v and observable rejection of dominant salt $\left(R_s^{obs}\right)$ are known. With these values and the Eq. 4 the membrane (P_s) $[m \cdot s^{-1}]$ and concentration-polarization layer $\left(P_s^{\delta}\right)$ $[m \cdot s^{-1}]$ permeabilities are calculated (3).

$$R_s^{obs} \equiv 1 - \frac{c_s^{"}}{c_s'} = \frac{\frac{J_v}{P_s}\exp\left(-\frac{J_v}{P_s^{\delta}}\right)}{1 + \frac{J_v}{P_s}\exp\left(-\frac{J_v}{P_s^{\delta}}\right)} \qquad \text{Eq. 4}$$

Where $c_s^{"}$ and c_s' are the concentration of the dominant salt in the permeate and feed solution $[mol \cdot m^{-3}]$, respectively.

2. Using Eq. 5 with the values of J_v and P_s, the intrinsic rejection of the dominant salt is obtained (R_s^{int}), and thus, the concentration of the dominant salt at the membrane surface ($c_s^{(m)}$)$[mol \cdot m^{-3}]$ (3).

$$R_s^{int} \equiv 1 - \frac{c_s^{"}}{c_s^{(m)}} = \frac{\frac{J_v}{P_s}}{1 + \frac{J_v}{P_s}} \qquad \text{Eq. 5}$$

3. Next, the concentration of trace ion at the membrane surface $\left(C_t^{(m)}\right)[mol \cdot m^{-3}]$ and thus, the intrinsic rejection of the trace (R_t^{int}) is calculated with Eq. 6 through the estimated value of concentration polarization layer thickness (δ) $[m]$ and the diffusion coefficients of ions $D_{\pm}^{(\delta)}$ $[m^2 s^{-1}]$ (3).

$$\frac{c_t^{(m)}}{c_t'} = \exp(Pe_t)\,[1 + R_s^{obs}(\exp(Pe_s) - 1]^{b^{\delta}} \cdot \left\{1 - \left(1 - R_t^{obs}\right)\int_{\exp(Pe_t)}^{1} \frac{dy}{\left[1 + R_s^{obs}(y^{-\alpha} - 1)\right]^{b^{\delta}}}\right\} \qquad \text{Eq. 6}$$

Where:

- c_t' is the concentration of the trace ion in the feed solution $[mol \cdot m^{-3}]$.
- c_t'' is the concentration of the trace ion in the permeate solution $[mol \cdot m^{-3}]$.
- y is a dummy integral variable $[-]$.
- $R_t^{obs} \equiv 1 - \frac{c_t''}{c_t'}$ is the observable rejection of trace ion due to membrane and concentration-polarization layer $[-]$.
- $R_t^{int} \equiv 1 - \frac{c_t''}{c_t^{(m)}}$ is the intrinsec rejection of trace ion due to membrane layer $[-]$.
- $\delta = \frac{D_s^{(\delta)}}{P_s^{(\delta)}}$ is the thickness of the concentration-polarization layer $[m]$.
- $D_s^{(\delta)} = \frac{(Z_+ - Z_-)D_+^{(\delta)}D_-^{(\delta)}}{Z_+ D_+^{(\delta)} - Z_- D_-^{(\delta)}}$ is the diffusion coefficient of dominant salt in concentration-polarization layer $[m^2 s^{-1}]$.

- $D_{\pm}^{(\delta)}$ are the diffusion coefficients of single ions of dominant salt in the concentration-polarization layer $[m^2 s^{-1}]$.
- $Z_{\pm}$ are the charges of single ions of the dominant salt.
- $Pe_s = \frac{J_v\,\delta}{D_s^{(\delta)}}$ is the Péclet number of the dominant salt.
- $Pe_t = \frac{J_v\,\delta}{D_t^{(\delta)}}$ is the Péclet number of the trace ion.
- $D_t^{(\delta)}$ is the diffusion coefficient of the trace ion in concentration-polarization layer $[m^2 s^{-1}]$.
- $b^{\delta} \equiv \frac{Z_t(D_+^{(\delta)} - D_-^{(\delta)})}{Z_+ D_+^{(\delta)} - Z_- D_-^{(\delta)}}\,[-]$.
- Z_t is the charge of the trace ion $[-]$.
- $\alpha = \frac{D_t^{(\delta)}}{D_s^{(\delta)}}\,[-]$.

4. When the particular case of single dominant salt and trace ions occurs, according to the SDM, the reciprocal intrinsic trans-membrane passage of a trace ion (f_t) can be represented as a function of reciprocal intrinsic trans-membrane passage of a dominant salt (f_s) as it is shown in Eq. 7 (3).

$$f_t = (f_s)^b + K\left(\frac{f_s - (f_s)^b}{1-b}\right) \qquad \text{Eq. 7}$$

Where:

- $f_t \equiv \frac{c_t^{(m)}}{c_t^{"}} = \frac{1}{1-R_t^{int}}\,[-]$.
- $f_s \equiv \frac{c_t^{(m)}}{c_s^{"}} = \frac{1}{1-R_s^{int}}\,[-]$.
- K and b are the parameters that need to be found mathematically.

5. Finally, the membrane permeabilities to single ions of dominant salt ($P_{\pm}$) $[m\,s^{-1}]$ can be estimated using Eq. 8 (3).

$$P_{\pm} = \frac{P_s}{1 - \left(\frac{Z_{\pm}}{Z_t}\right) b} \qquad \text{Eq. 8}$$

And the membrane permeability to trace ions (P_t) $[m\ s^{-1}]$ can be estimated with Eq. 9 (3).

$$P_t \equiv \frac{P_s}{K} \qquad \text{Eq. 9}$$

Following the prior steps a modeling of the rejection behaviour for each membrane is obtained as well as the permeabilities of both dominant salt and trace ions.

4. Methodology

4.1. Groundwater

The groundwater that was used for this project was extracted the 26th of March, 2019. The geographic location is detailed in Figure 12 (extracted from the study carried out by Anna Jurado et al. (1)). The pumping well were the water was extracted was SAP-1 (green circle (b)) at a depth of approximately 10 meters.

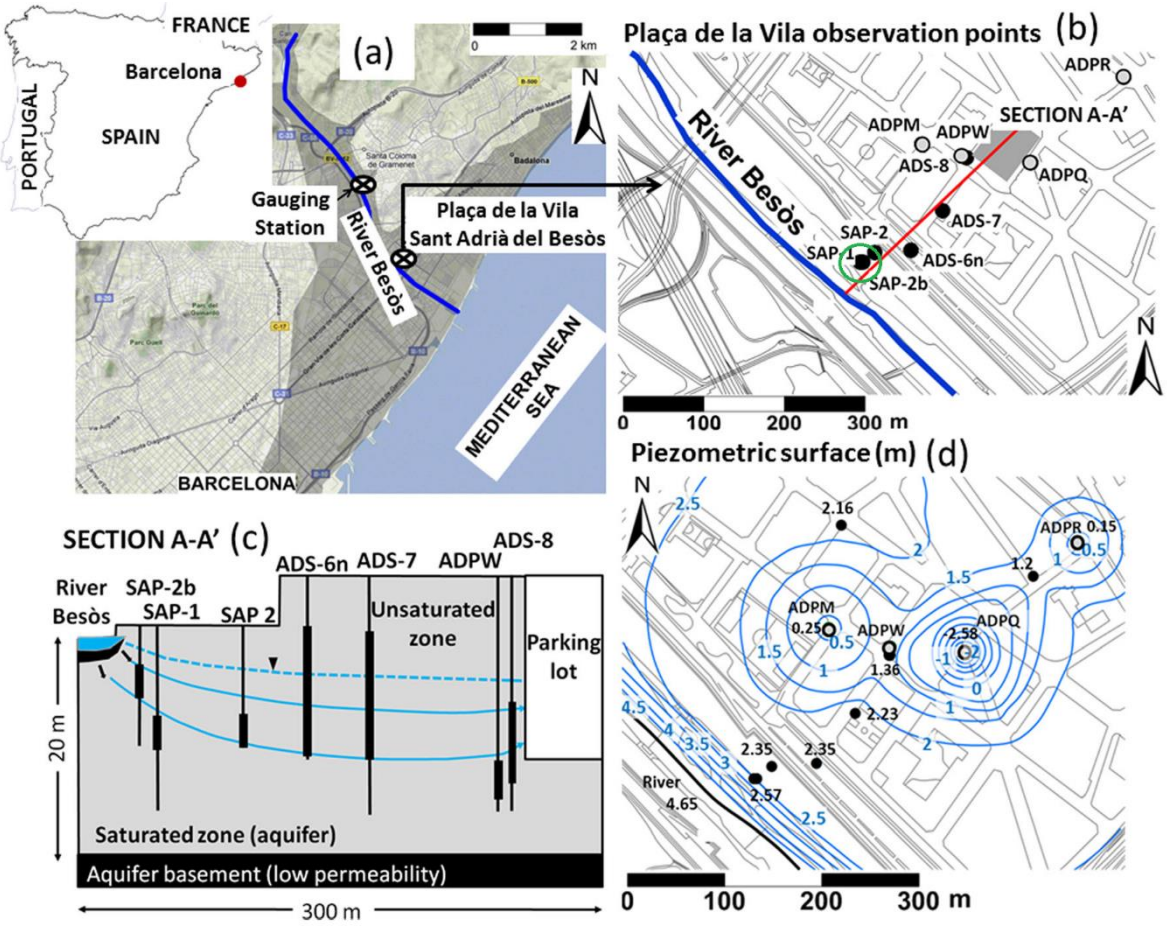

Figure 12. (a) Location of the study area and (b) spatial distribution of the observation points (section A–A'). (c) Schematic description of the hydrogeological conceptual model as well as the screen depths of the pumping well and the observation points. (d) The piezometric surface from the River Besòs to the parking area. Note that the piezometric level is in meters above the sea level. (1)

4.2. Membranes

For this project three commercial polyamide-based NF membranes where used: NF270, NF90 and DL. One of the characterization methods used with filtration membranes is the Molecular weight cut-off (MWCO). This method describes the retention capabilities and pore size distributions of membranes. Its definition, although not standardized, is the lowest molecular weight, measured in Daltons, at which more than 90% of a solute with known molecular weight is impeded by the membrane.

4.2.1. NF270

It is a polyamide thin-film composite membrane (Figure 13) that removes a high percentage of total organic carbon (TOC) and trihalomethane precursors while having a medium to high salt passage and medium hardness passage. In continuous operation mode it can treat water with pH ranging from 2 to 10. Maximum operating temperature is 45°C and maximum temperature for continuous operation above pH 10 is 35°C (36). The MWCO is 200-300 Da (37). IEP is expected to be around 3 (38). The functional groups that become deprotonated are carboxylic acid and secondary amine. This membrane was provided by Dow Chemical Company.

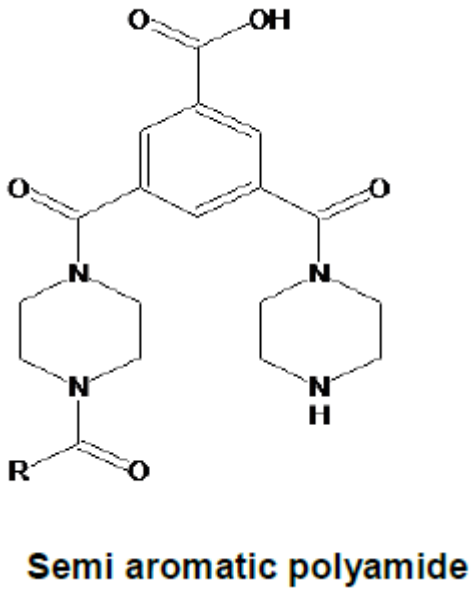

Figure 13. NF270 composition of the active layer

4.2.2. NF90

It is a polyamide thin-film composite membrane (Figure 14) that removes a high percentage of salts, nitrate, iron and organic compounds such as pesticides, herbicides and THM precursors. The low net driving pressure of the NF90 membrane allows the removal of these compounds at low operating

pressures. In continuous operation mode it can treat water with pH ranging from 2 to 11. Maximum operating temperature is 45°C and maximum temperature for continuous operation above pH 10 is 35°C (39). The IEP is around 4 (40). The MWCO is 200-400 Da (41). The functional groups that become deprotonated are carboxylic acid and amine (primary and secondary). This membrane was provided by Dow Chemical Company.

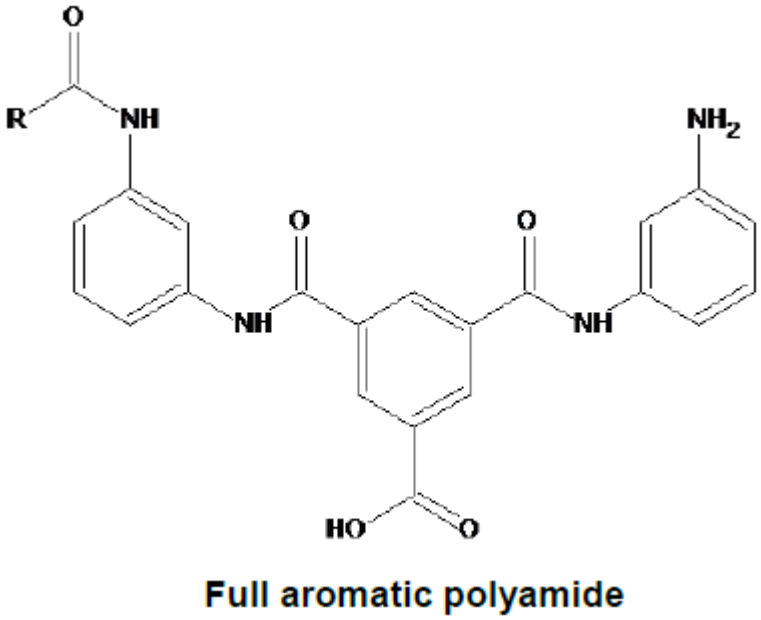

Figure 14. NF90 composition of the active layer

4.2.3. DL

It is a polyamide based membrane that shows similar behaviour with NF270, but according to manufacturers it incorporates another polyamide layer that influences its properties. However they do not share similar IEP because DL presents an IEP of 5 (42). Its MWCO is 150-300 Da (43) and It presents high metal and sulphate rejections (42). The functional groups that become deprotonated are carboxylic acid and amine. This membrane was provided by GE Power.

4.2.4. Membrane comparison

In Table 5 the main differences of the membranes used in this project are summarized.

Table 5. Comparison of membrane properties.

Membrane	Functional groups	pH ranges for continuous operation	Maximum operating temperature	Iso-electric point	MWCO (Da)
NF270	carboxylic acid, amine (secondary)	2-10	45 °C	3	200-300
NF90	carboxylic acid, amine (primary and secondary)	2-11	45 °C	4	200-400
DL	carboxylic acid, amine	3-9	50 °C	5	150-300

4.3. Operation method

The experiments were carried out in cross flow mode using a FS module and a membrane with an effective surface area of 0,014 m^2 (Figure 15).

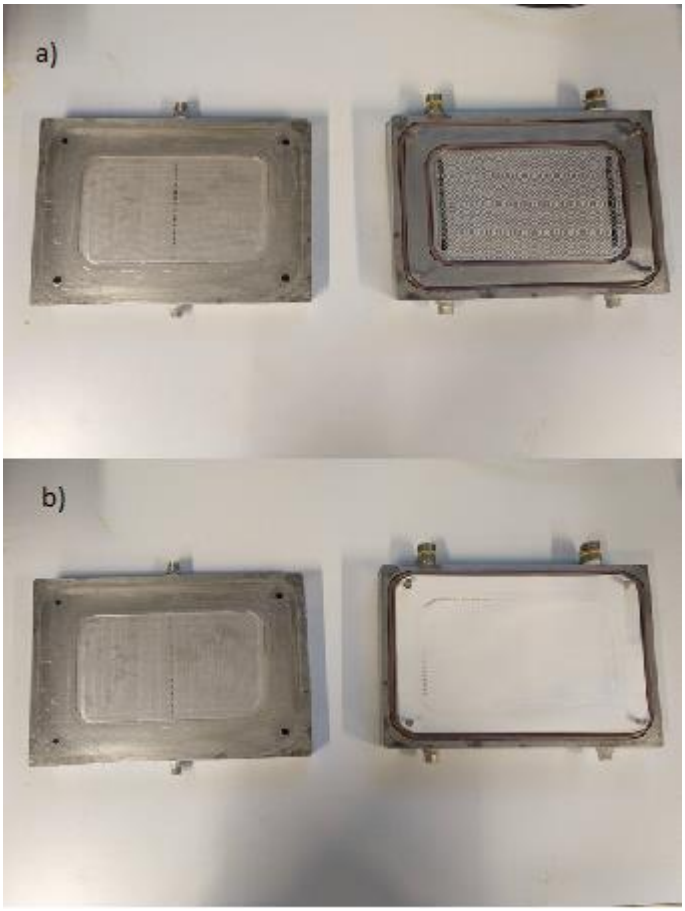

Figure 15. Flat sheet module with spacers and O-rings without membrane (a) and with membrane (b)

4.4. Experimental setup

4.4.1. Plant schematics

Water extracted from the underground area of the Besòs was used for this experiment. The experimental set-up used is shown in Figure 16. The solution was placed in a refrigerated tank (30L) (Figure 17) and was kept at a temperature of $20 \pm 2°C$ during the experiment. The feed solution was introduced in the filtration unit using a pump at a constant flow rate, measured with a flow meter (Figure 18). The feed concentration was kept constant due to the constant recirculation of the output flows: permeate and concentrate. The by-pass (Figure 19) and the needle valves (Figure 20) controlled the variation of the TMP and the cross flow velocity (CFV). The TMP was measured by calculating the average of the 2 pressure gauges (Figure 21). Finally, a pre-filter cartridge (Figure 22) was put in the concentrated stream to avoid fouling and protect the membrane.

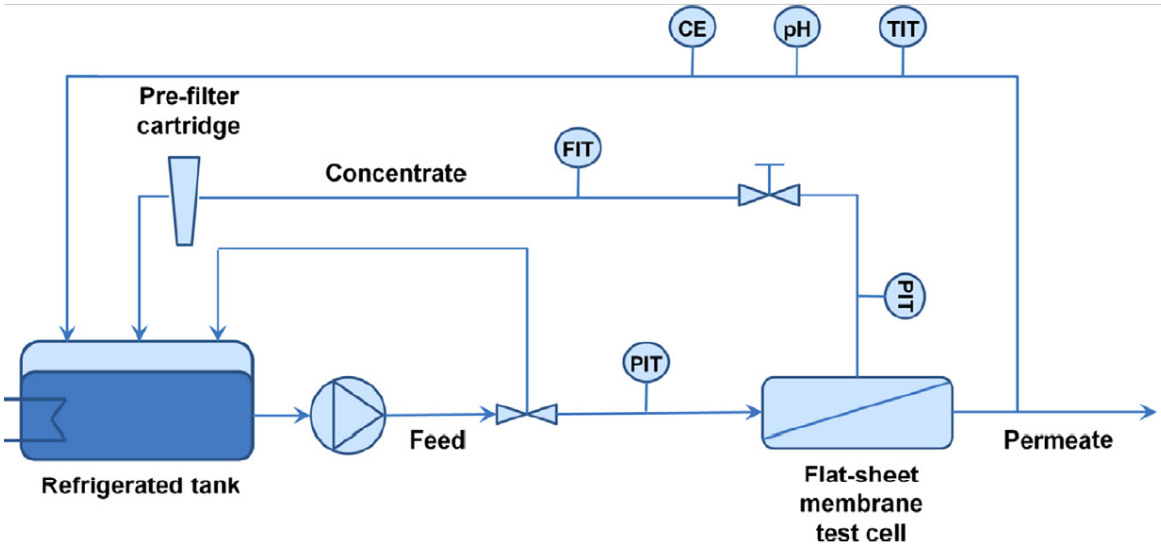

Figure 16. Experimental set-up (3)

Where:

- PIT = Pressure measurement point
- FIT = Flow measurement point
- CE= Conductivity meter
- pH = pH-meter
- TIT= Temperature measurement point

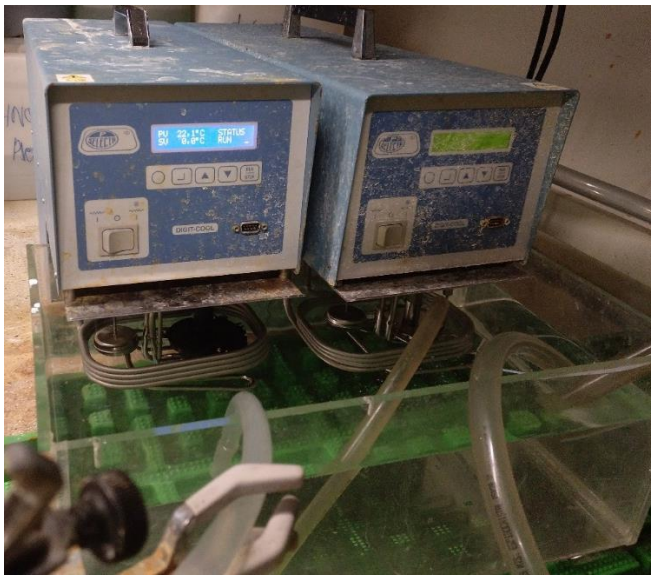

Figure 17. Refrigerated tank

Figure 18. Flow meter

Figure 19. By-pass valve

Figure 20. Needle valve

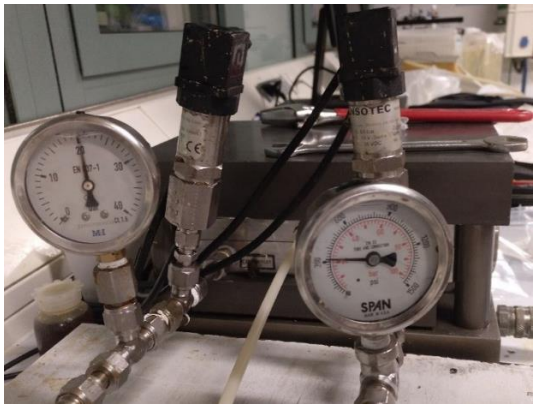

Figure 21. Pressure gauges measuring the concentrate (left) and the feed (right)

Figure 22. Pre-filter cartridge

4.4.2. Procedure

Before starting the experimental procedure the NF membrane is put in Milli-Q water for 24 hours to remove its preservative products. Afterwards, the FS module is set positioning the O-rings, the spacers and then laying the membrane (Figure 15). Once the module is ready, it gets connected to the hydraulic system through the feed, permeate and concentrate pipes. Subsequently, the module gets pressurized to 40 bar with a manual pump. Now the refrigerators turn on and so does the pump. The pump operates at 38 Hz. This value must be achieved gradually, allowing the pump to get rid of the air that could be inside. The system is now ready and it only needs to be set at the desired pressure and flow using the tap and needle valves.

Once the filtration process has already begun and in order to prevent problems that could jeopardize the whole experiment, every 15 min the pH, temperature and electric conductivity are measured. This

way if odd values are detected the possible causes can be addressed such as membrane misplacement or breakage.

The procedure is divided in four section:

4.4.2.1. Pressurization of the membrane with water

Using distilled water as feed, the system was put in motion for 2 hours in order to pressurize the membrane. The CFV was kept constant at 5 $\frac{L}{min}$ and the TMP was of 32 bar the first 90 minutes and 22 bar the last 30 minutes

4.4.2.2. Pressurization of the membrane with solution

This stage is done using the same parameters as 4.4.2.1 but already using the Besòs water solution.

4.4.2.3. Experiment

During the experiment the CFV was kept at 3,46 $\frac{L}{min}$ and the TMP was gradually changed from 6 bar to 32 bar. Samples were collected every 7 minutes. Once a sample was collected, the TMP was raised and the system was left to stabilize until the next sampling. For every experiment 13 permeate and 2 feed samples were taken.

4.4.2.4. Cleaning

In order to clean the whole system and the membrane, the solution was extracted from the tank and distilled water was put instead. Two cleaning cycles were done per experiment (30 minutes and 90 minutes), between cycles the distilled water was replaced. The first cycle operated at 10 bar TMP and the second at 22 bar. Both of them had a CFV of 5 $\frac{L}{min}$.

4.4.3. Design of the experiment

The experimental part of this project is based on the results obtained from 3 NF membranes (4.2). The same feed solution was used for all the experiments and for each type of membrane 2 experiments were done, making a total of 6 experiments. The membrane was always replaced by a new one in order to avoid fouling from prior experiments.

4.5. Analysis methods

The parameters that were measured were pH, electrical conductivity and ion concentrations. Experimental samples were analysed using three different methods.

4.5.1. pH meter

The equipment used for the determination of the acidity levels was a pH meter GLP 22 provided by Crison.

4.5.2. Conductivity meter

The equipment used for the measurement of electrical conductivity was EC-Metro GLP 31 provided by Crison.

4.5.3. Ion chromatography

The equipment used was an ionic chromatograph system (Dionex ICS-1000 and ICS-1100 Thermo-Fisher Scientific, USA), equipped with ICS-1000 and ICS-1100 cationic and anionic detectors, respectively, and controlled by using Chromeleon® chromatographic software. For the ion chromatographic quantification, a CS16 column (4×250 mm) and an AS23 column (4×250 mm) (Phenomenex, Barcelona, Spain) were used for cation and anion determination, respectively. The mobile phase was a 0,03 mol/L CH3SO3H solution for cations and a mixture of 0.8 mmol/L $NaHCO_3$ and 4,5 mmol/L Na_2CO_3 for anions. Ionic chromatography was used to measure the following analytes: Na^+, NH_4^+, K^+, Mg^{2+}, Ca^{2+}, F^-, Cl^-, Br^-, NO_3^-, PO_4^{3-}, SO_4^{2-}. Detection limits were not stated in the operation manual or specifications. However, standard curves were built and the limit of detection was found using analyte-free samples of Milli-Q water in order to quantify the noise signal. For ammonium, the ion of interest with lower concentration, the detection limit was established at 0,2 ppm.

4.5.4. Mass spectrometry

Inductively coupling plasma mass spectrometry (ICP-MS) was used to determine elements in the µg/L concentration range (Elan 6000, Perkin Elmer) (44). It was used to measure the concentration of B, Al, Cr, Mn, Fe, Ni, Cu, As, Cd, Pb. The detection limits for each element were Al (58 parts per trillion (ppt)), Cr (2 ppt), Fe (2 ppt), Ni (5 ppt), Cu (1,7 ppt), As (22 ppt), Cd (7 ppt) and Pb (0.8 ppt).

4.5.5. Titration

For the HCO_3^- determination, the equipment used was an autotitrator model T70/Rondolino and controlled with LabX titration software. All samples to be determined had pH ranges that induced HCO_3^- as the controlling compound of the bicarbonate ion. In order to quantify it, hydrochloric acid was

used as titrator and added until the solution reached the equivalence point. No chemical indicator was used. Throughout the determination, the added volume of titrator was measured; knowing the volumes used of both titrator and sample, and the titrator concentration, the HCO_3^- concentration of the sample was calculated.

5. Results

This section is based on the measured trans-membrane fluxes and the analysis results obtained from ion chromatography and ICP-MS. With these values, R_s^{obs} and R_t^{obs} were calculated and with them, the SDFM was built.

All three membranes had a lower IEP than the pH of the solution they were exposed to. Hence, their active layers were deprotonated and thus, presented a negative surface charge that favoured the transport of cations while the ones for anions was impeded.

5.1. Assessment of the groundwater quality

Groundwater tends to be under a lesser oxidizing environment than the surface. Therefore, chemical species that are usually found in oxidized states at the surface may be found in reduced states below the surface. A case in point is iron (2.3.2) which is found dissolved with a +2 oxidation state in reducing environments and precipitates easily when exposed to oxidizers.

The analysis of the samples was elaborated off-site. Electrical conductivity and pH values varied from 1288 to 1779 µS/cm and from 7,7 to 8,4, respectively. Nevertheless pH values may be differ from in-site analysis, being probably lower in the off-site analysis. This is because in an oxidizing atmosphere metals (M) precipitate more than they would in a reducing one, therefore reducing the number of OH^- groups and thus lowering the pH levels.

$$M^{n+}(\text{aq}) \xrightarrow[Oxidation]{} M^{m+}(\text{aq}) \xrightarrow[Precipitation]{} \text{M}(OH)_m(s) \downarrow$$

5.1.1. Composition

Besides the study of the underground water compositions of the Besòs area carried out by Anna Jurado et al. (1) (detailed in 2.3) an independent analysis was carried out by the author to ascertain the similarity of both results.

Table 6. Average concentration of major ions in ppm. Note that Cm is the average concentration and RD 140/2003 are the recommended limits for Spanish drinking water guidelines.

Chemical parameter	C_m by the author	C_m (2.3)	Variation (%)	RD 140/2003
Sodium	175,2	175,6	0,2%	200

Ammonium	0,3	5,1	94,1%	0,5
Potassium	18,3	17,9	2,2%	-
Magnesium	54,6	26,9	103,0%	-
Calcium	198,1	128,7	53,9%	-
Fluoride	0,3	-	-	-
Chloride	335,2	229,0	46,4%	250,0
Bromide	0,5	-	-	-
Nitrate	12,9	3,9	230,8%	50,0
Sulfate	139,0	155,8	10,8%	250,0
Bicarbonate	384,4	419,1	8,3%	-

Table 7. Average concentration of hazardous metals in ppb. Note that Cm is the average concentration and RD 140/2003 are the recommended limits for Spanish drinking water guidelines.

Chemical Parameter	C_m by the author	C_m (2.3)	Variation (%)	RD 140/2003
Boron	157,9	224,8	29,8%	1000,0
Aluminium	29,6	53,0	44,2%	200,0
Manganese	141,6	258,0	45,1%	50,0
Nickel	12,1	5,0	142,0%	20,0
Copper	6,5	3,9	66,7%	2000,0
Arsenic	126,0	11,7	976,9%	10,0
Lead	0,7	1,1	36,4%	10,0
Cadmium	0,1	0,4	75,0%	5,0

Chromium	<Detection limit	8,6	-	50,0
Iron	<Detection limit	423,1	-	200,0

When comparing the results of both analyses the following difference stand out:

- **Ammonium**: The prior study detected concentrations well over the drinking limit while the analysis carried out by the author determined that the concentrations were below that limit. This could be attributed to seasonal changes of the groundwater settlement of the Besòs area or the degradation of ammonia occurred during the experiments, when the feed solution was exposed to air in conditions that facilitated its evaporation.
- **Chloride**: Concentrations from the author analysis were higher than the drinking limit while the ones of the other study were not.
- **Iron**: The water concentration of iron was over the limit according Jurado et al. (1) whereas below detection limit in this study. This result could be explained by the reduced oxidation state iron is found in underground waters where it is in a dissolved condition. Whereas when exposed to the surface environment, iron is oxidized (2.3.2) and precipitates, leaving the water concentration of dissolved iron with a value close to zero.
- **Arsenic**: Both studies found values over the drinking limit. However, the analysis carried out by the author showed concentrations higher by one power of ten those of Jurado et al. (1).

It should be kept in mind that these differences can be explained by changes in the underground water composition due to variations of the state of the inflows or seasonal changes. The state of the elements in solution is shown in Table 8.

Table 8. State of the elements in solution at pH 7,5.

Element	Speciation in solution
Sodium	Na^+ (100%)
Ammonium	NH_4^+(98,5%) and $NH_3(aq)$(1,5%)
Potassium	K^+ (97%), KSO_4^-(3%)
Magnesium	Mg^{2+} (100%)
Calcium	Ca^{2+} (91%) and $CaSO_4(aq)(9\%)$

Fluoride	F^- (100%)
Chloride	Cl^- (100%)
Bromide	Br^- (100%)
Nitrate	NO_3^- (100%)
Sulfate	$SO_4^{2-}(75\%)\ and\ CaSO_4(aq)(25\%)$
Bicarbonate	H_2CO_3(3%), HCO_3^- (89%), CO_3^{2-}(1%), $CaCO_3(aq)$(7%)
Boron	H_3BO_3 (100%)
Aluminium	$Al(OH)_3$ (100%)
Manganese	Mn^{2+} (100%)
Nickel	Ni^{2+} (100%)
Copper	Cu^{2+} (>79 %) and $CuSO_4(aq)(21\%)$
Arsenic	H_3AsO_3 (100%)
Lead	$Pb(OH)_4$ (100%)
Cadmium	Cd^{2+} (100%)

5.2. Trans-membrane flux dependence to trans-membrane pressure

Increasing the TMP makes the trans-membrane flux (J_v) to boost. While this issue could be of apparent knowledge to the reader, it is not the fact that they have a lineal dependency as it is shown in Figure 23. From it, it can also be deduced that the 3 membrane have different J_v across the same TMP values. It is important to know these graphics when trying to build up an industrial scale plant due to the fact that higher J_v means more volume of treated water (NF270>NF90>DL). The water permeability values obtained at 32 bar for the NF270, NF90 and DL are 2,60; 1,68 and 1,52 $\frac{\mu m}{s \cdot bar}$, respectively.

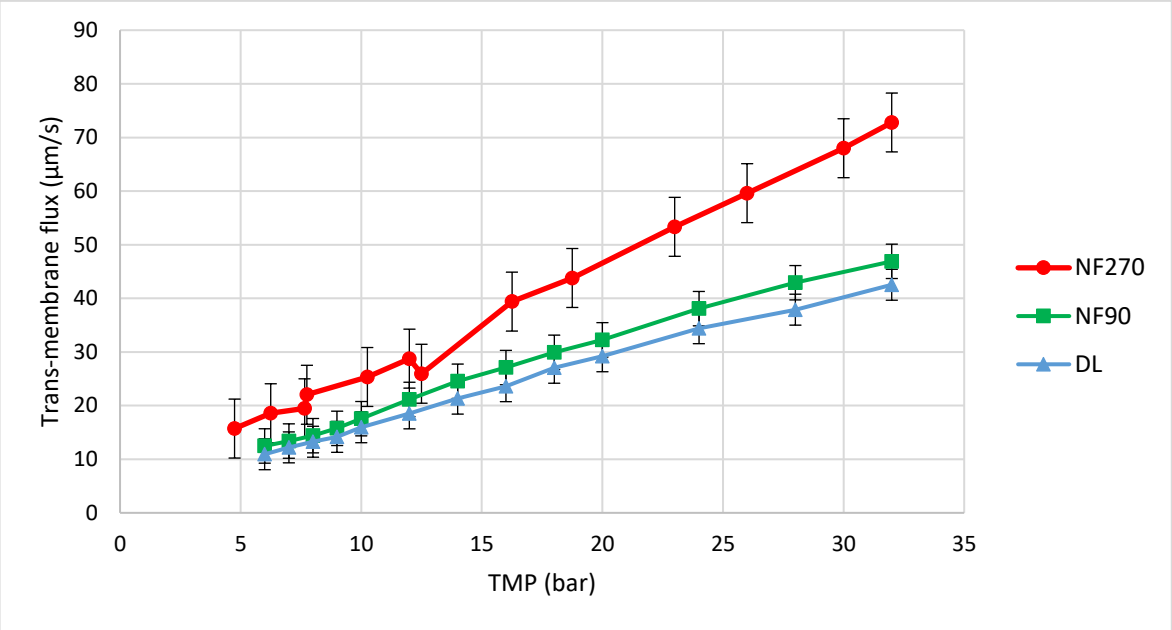

Figure 23. Trans-membrane flux vs TMP

5.3. Dominant salt rejection

Due to always using the identical feed solution for all experiments, the dominant salt (NaCl) was always the same. As stated before (Solution-Diffusion-Film Model), the intrinsic rejection determines the ion removal from the membrane surface, whereas the observable rejection from the feed solution.

NF270 (Figure 24) and DL (Figure 25) rejected a similar amount of NaCl, although NF270 rejections were slightly higher, around 5% more across the trans-membrane flux domain.

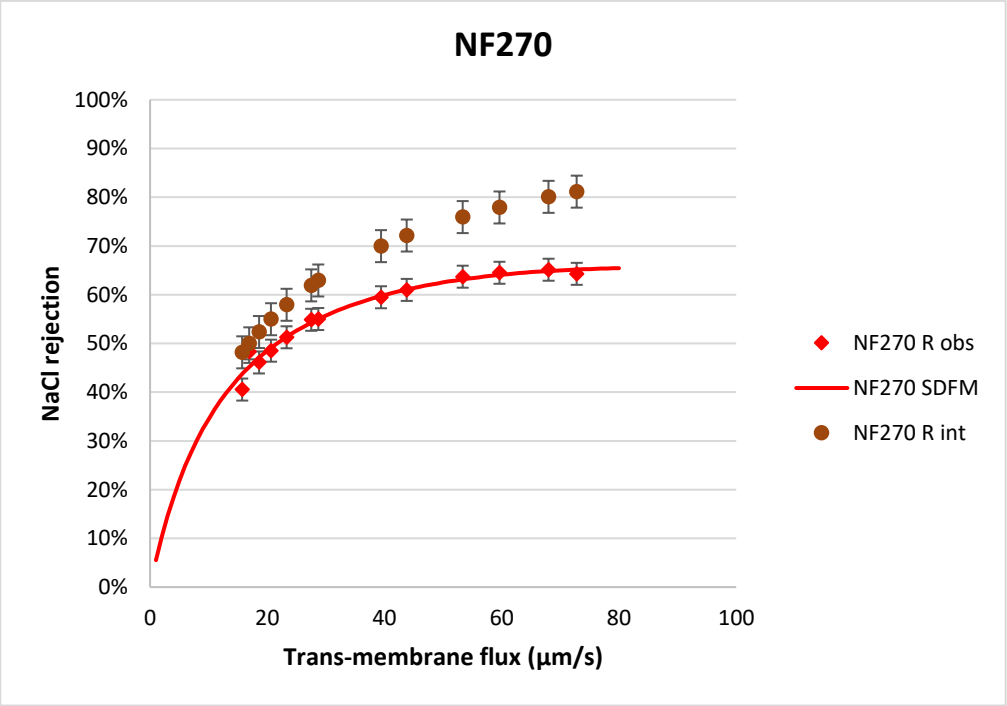

Figure 24. NF270 dominant salt rejection

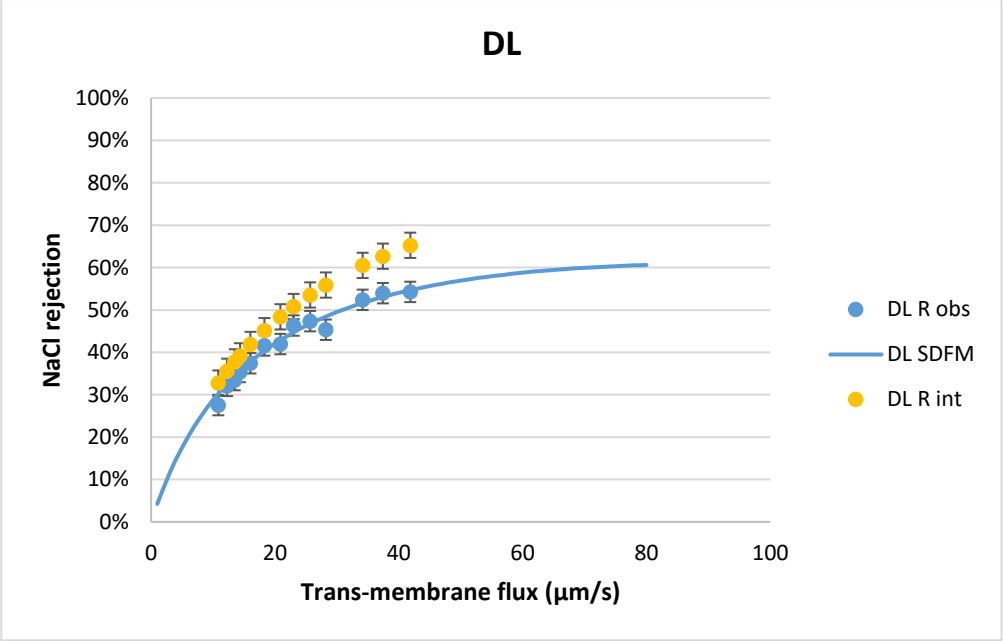

Figure 25. DL dominant salt rejection

NF90 (Figure 26) achieved fairly higher values of dominant salt rejection than NF270 and DL, achieving values of more than 90% in all the experimental measurements.

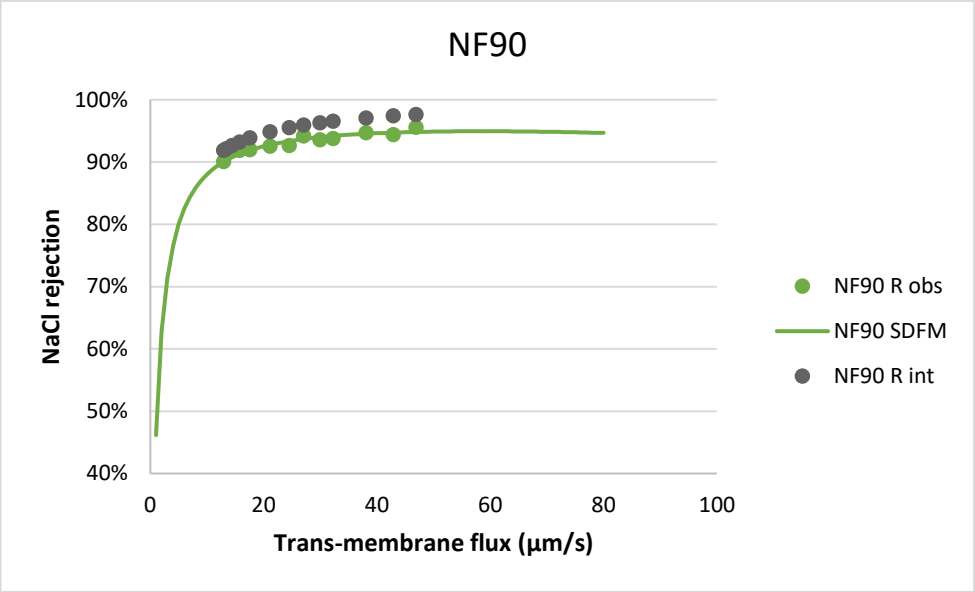

Figure 26. NF90 dominant salt rejection

For all membranes, the values of R_s^{int} were always higher than R_s^{obs}. This result was expected due to the existence of a concentration-polarization layer (2.6.4) that makes the salt concentration at the membrane $C_s^{(m)}$ higher than the feed concentration C_s'.

5.4. Trace ions rejection

For each membrane two graphics of trace ions were made. This differentiation was made to establish a more clear representation of the rejection curves and to divide the ions of interest in groups of similar concentrations. Being that cleared out, the ion set with concentrations of ppm is: $SO_4^{2-}, Mg^{2+}, Ca^{2+}, HCO_3^-$, NH_4^+, Br^-, K^+ and NO_3^-; and the set with ppb concentrations, which happens to be the one formed with heavy metals and metalloids, is: $Al^{3+}, Cu^{2+}, Pb^{2+}, As^{3+}, Ni^{2+}, Mn^{2+}$ and B^{3+}.

5.4.1. NF270

Figure 27 shows two different groups of ions in quantitative rejection terms. One with rejections higher than 70% ant the other with rejections lower than 55%. The first one includes, in descending order of rejection $SO_4^{2-}, Mg^{2+}, Ca^{2+}, HCO_3^-$; the best rejected ions happen to be all divalent which concurs with the theory, stated before in 2.4 and explained with the phenomenon of dielectric exclusion in 2.6.2, that divalent and trivalent ions are rejected better than monovalent ones. Besides, the ion best rejected (99%) is SO_4^{2-}, a counter-ion, due to the Donnan exclusion phenomenon (2.6.1). Moreover, the SDFM model shows good fit with the experimental data.

The second group includes, also in descending order of rejection $NH_4^+, Br^-, K^-, NO_3^-$; these ions are monovalent and thus, are less rejected by the membrane. The rejection values range from 5% to 55% making this membrane poorly effective against these ions, especially nitrate which at maximum trans-membrane flow experiences a rejection of 20%.

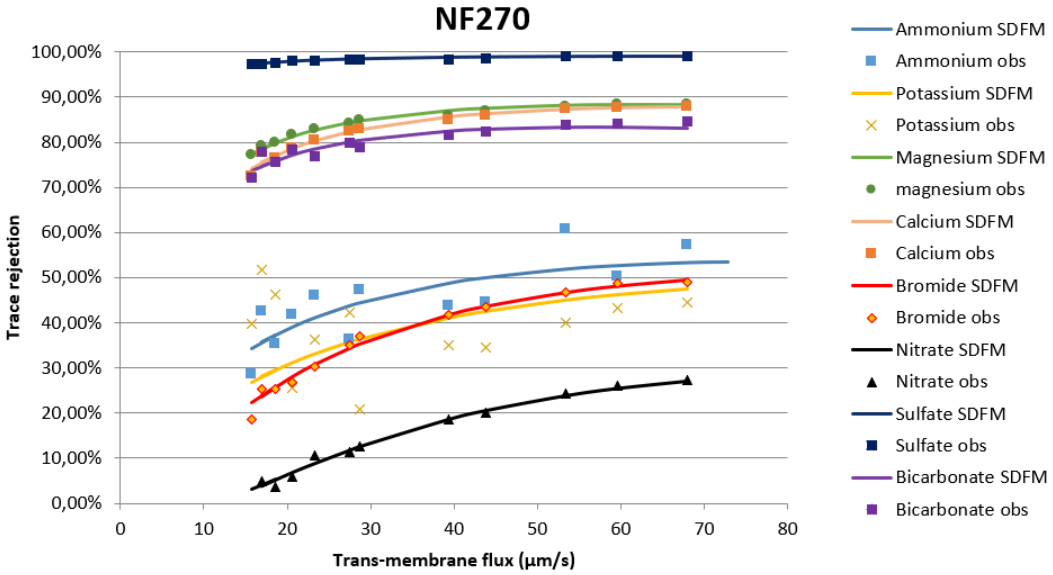

Figure 27. NF270 trace ions rejection

Figure 28 shows the rejection of heavy metals. In it, it can be observed that there are metals excellently rejected, with rejection values higher than 95%. These are, in descending order of rejection $Al^{3+}, Cu^{2+}, Pb^{2+}, As^{3+}$. As for Ni^{2+}, Mn^{2+} *and* B^{3+} their rejection values oscillate from 75% up to 92%.

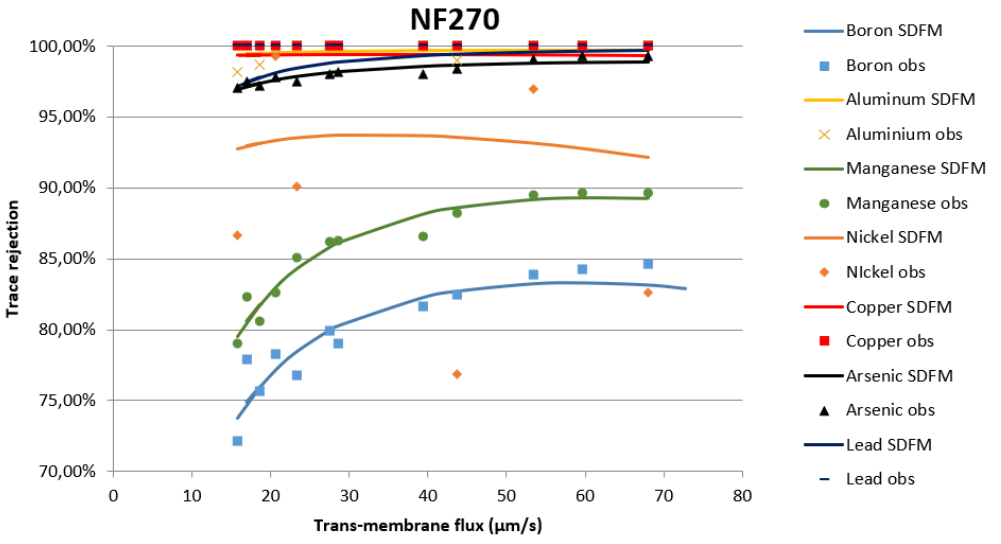

Figure 28. NF270 trace metal ions rejection

5.4.2. NF90

The membrane NF90 has a behaviour more similar to RO than NF membranes due to its generally high salt rejections. Even though, there are still notable differences regarding divalent and monovalent rejections.

As Figure 29 illustrates, $SO_4^{2-}, Mg^{2+}, Ca^{2+}, HCO_3^-$ *and* Br^- ions experience rejections of more than 98%; while NH_4^+, K^- *and* NO_3^- ions have, although lower rejections, ranging values from 60% to 90%.

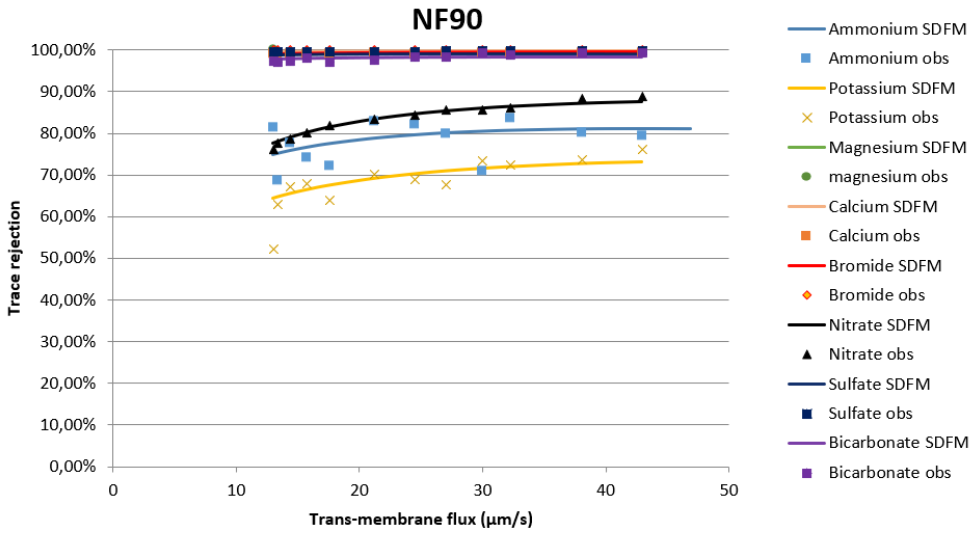

Figure 29.NF90 trace ions rejection

As can be seen in Figure 30, all heavy metal traces but two have rejections higher than 95%. Those two are lead and arsenic, and they experience rejections of 87% and 82%, respectively, at their maximum trans-membrane flux.

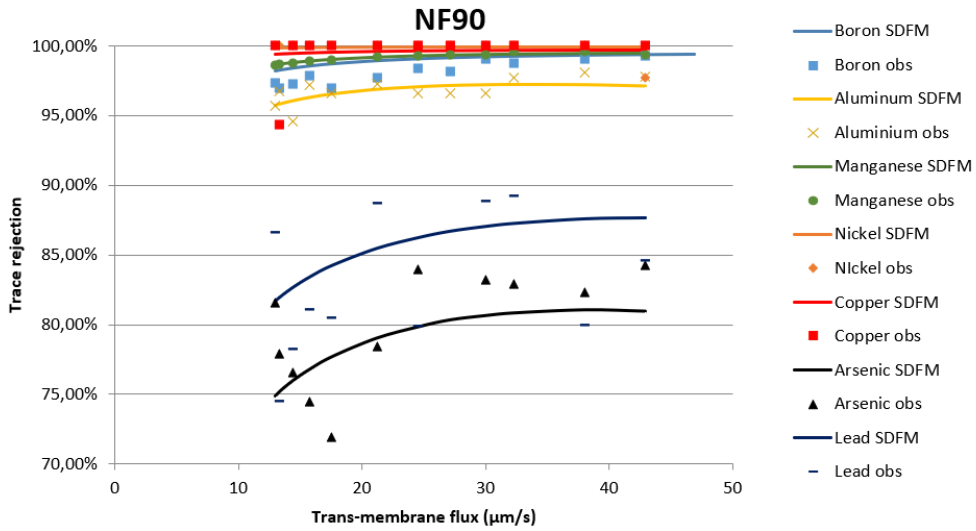

Figure 30. NF90 trace metal ions rejection

5.4.3. DL

As stated in 4.2.3, DL and NF270 membranes share similarities in their rejection behaviour. DL membranes also reject better divalent ions, and similarly to NF270, although with a notable drop in the rejection of HCO_3^- which was rejected at around 80% using NF270 and is rejected at around 60% with the DL membrane. However, $NH_4^+ \; and \; NO_3^-$ rejections were 20% higher using DL instead of NF270.

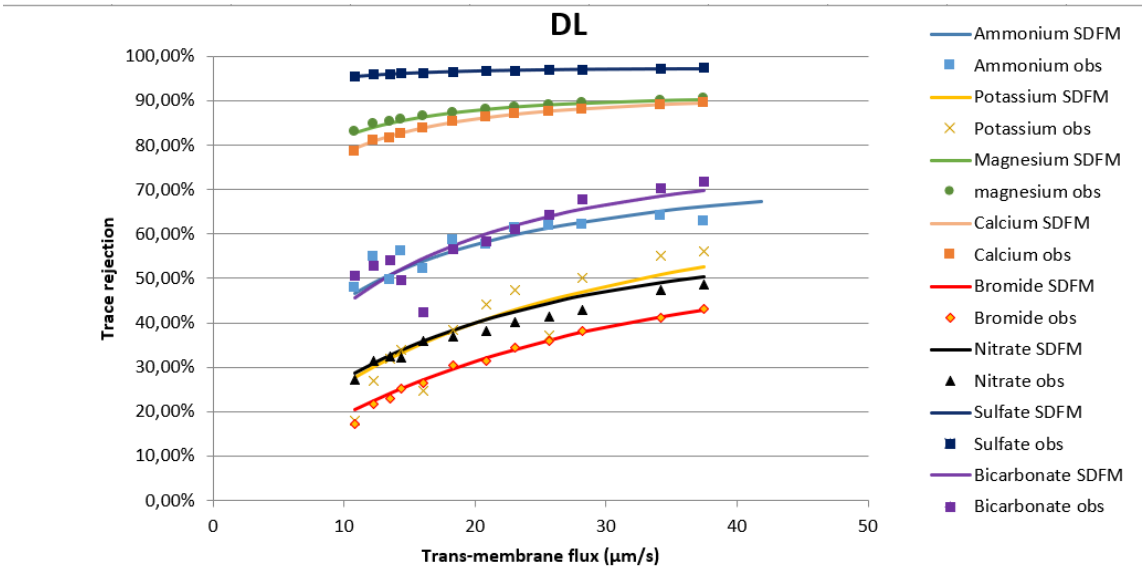

Figure 31. DL trace ions rejection

The graph below (Figure 32) shows a more even panorama of rejections, although quantitatively lower than those of NF270 and NF90. DL rejects better, in decreasing order, the following metals: $Cu^{2+}, Al^{3+}, Mn^{2+}, As^{3+}, Ni^{2+}, Pb^{2+} \; and \; B^{3+}$.

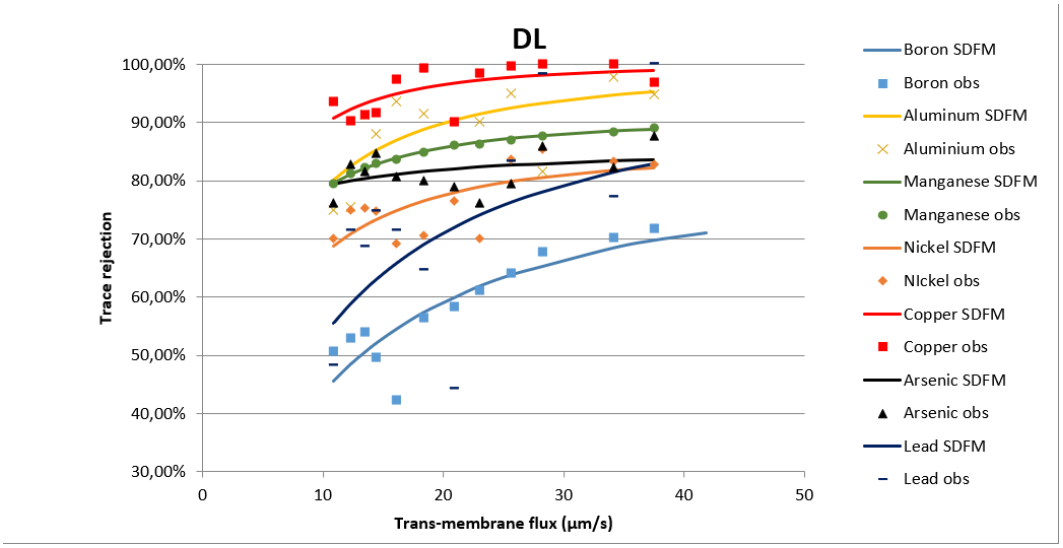

Figure 32. DL trace metal ions rejection

5.4.4. Trace ion rejections comparison

When comparing the rejections of the three membranes, it is clear that the rejections of divalent and trivalent ions, for similar feed concentrations, are higher than the monovalent ones. This fact proves the veracity of the dielectric exclusion. However, trivalent ions (only found at ppb concentrations) which should be rejected better than divalent ones, according to the dielectric exclusion, are not. This is due to the fact that trivalent ions are found at far lower concentrations than divalent ions.

Taking into account only the ions with concentrations values of ppm, the NF90 has the best rejection values for each ion. Aside, NF270 and DL have fairly the same rejection values, except for bicarbonate which is better rejected by NF270 (83%); and for ammonium and nitrate rejection where DL works better (67% and 52%, respectively).

When looking into the ions with concentrations values of ppb (heavy metals and metalloids), the membranes NF270 and NF90 have similar rejections. For NF90, all metals were rejected at more than 95%, excepting arsenic and lead which ranged from 75% to 81%, and from 82% to 88%, respectively. On the other hand, for NF270, all metals were also rejected at more than 95%, excepting nickel (92%), manganese (from 80% to 89%) and boron (from 75% to 83%). As for the DL membrane, their rejections were lower (up to a maximum of 20%) for every ion but arsenic (from 80% to 84%), which experienced slightly higher rejections than those of NF90.

The NF90 has a higher global rejection than the other two, followed by NF270 and finally DL.

Table 9 shows the rejections obtained using the SDFM at TMP 32 bar. At this pressure, the rejections are at their peak values.

Table 9. Ion rejections at 32 bar.

Species	NF270	NF90	DL
$\boldsymbol{Na^+}$	66%	95%	53%
$\boldsymbol{Cl^-}$	63%	96%	55%
NH_4^+	53%	81%	67%
K^+	48%	73%	55%
Mg^{2+}	88%	99%	90%
Ca^{2+}	88%	100%	90%

Br^-	50%	100%	45%
NO_3^-	28%	88%	52%
SO_4^{2-}	99%	99%	97%
HCO_3^-	83%	98%	71%
B^{3+}	83%	99%	71%
Al^{3+}	100%	97%	96%
Mn^{2+}	89%	99%	89%
Ni^{2+}	92%	100%	82%
Cu^{2+}	99%	100%	99%
As^{3+}	99%	81%	84%
Pb^{2+}	100%	88%	85%

Focusing on the bicarbonate ion, it is the conjugated base (from the carbonic acid) with the highest concentration of all the conjugated bases present. Having all three membranes a notable rejection of this ion, it should be taken into account the variation of the pH that this situation creates. When HCO_3^- is rejected, and also the small amounts presents of CO_3^{2-} (rejected at a higher rate due to dielectric exclusion), the equilibrium with H_2CO_3 gets disrupted. In order to recover the status of equilibrium, the carbonic acid dissociates itself and thus, procures more protons to the solution, lowering the pH.

$$H_2CO_3 \leftrightarrow HCO_3^- + H^+ \qquad pK_a = 6,3$$

$$HCO_3^- \leftrightarrow CO_3^{2-} + H^+ \qquad pK_a = 10,3$$

To quantify this effect the pH values of both feed and permeate were measured, being the average pH of the feed solution 8,1 and the average pH of the permeate 7,2. Figure 33 shows that, at these pH values, the controlling ion is the bicarbonate.

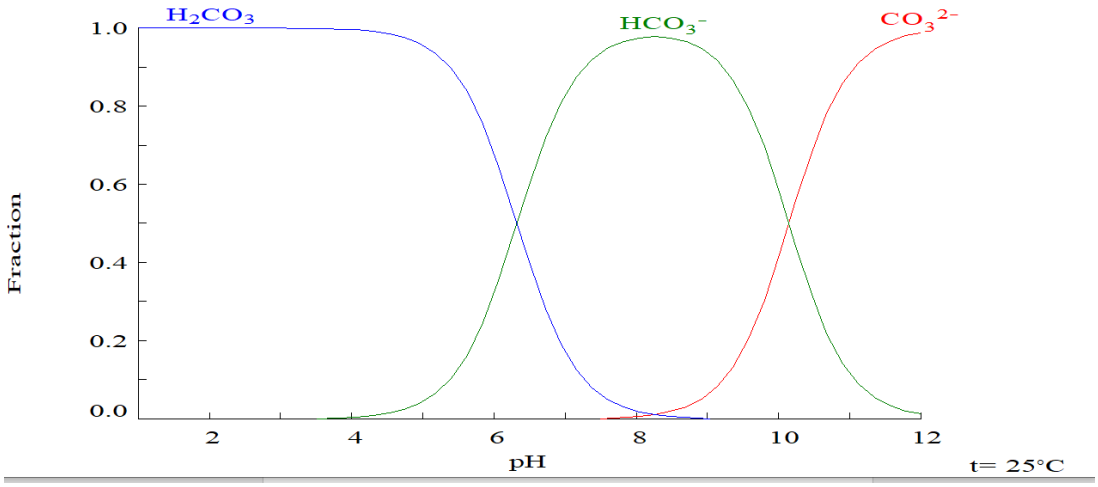

Figure 33. Fraction diagram of the acid carbonic

Figure 34 illustrates how changes in trans-membrane flux affect the pH. The graphic shows a prompt drop in pH levels at early permeate samples, and afterwards, a slightly downward trend as the TMP raises. All three membrane experiments started with a pH of around 8,1 due to the fact that all used the same feed solution. The NF270 produced the lowest pH variation (-0,5) followed by the DL (-0,8); the NF90 caused the highest pH shift (-1,2).

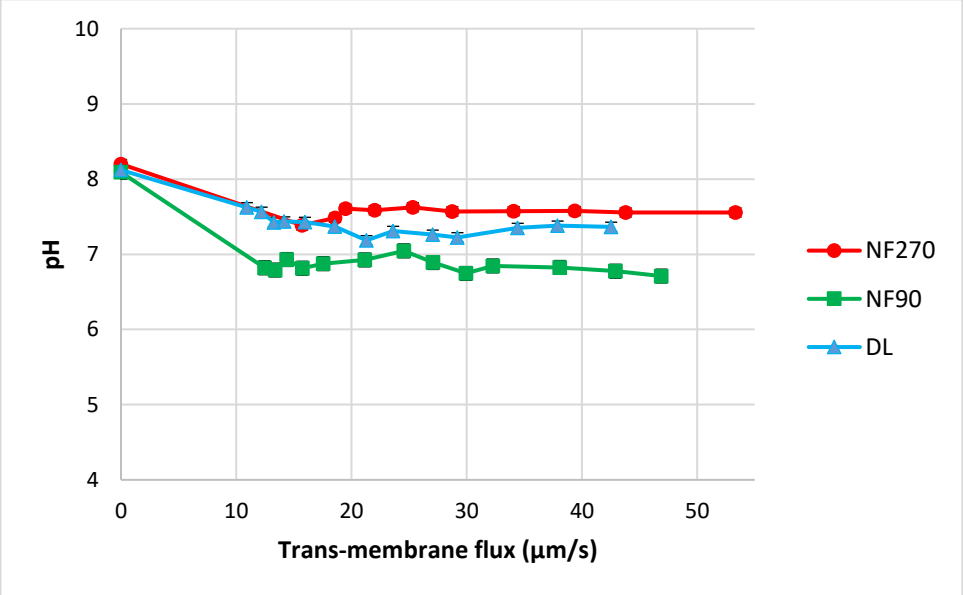

Figure 34. Evolution of pH as a function of trans-membrane flux

5.5. Ion permeabilities

For the calculation of the permeabilities (Table 10) the SDFM model was used (5). As Eq. 9 shows, the permeability of the trace ion is directly proportional to the dominant salt permeability and inversely proportional to the mathematical K parameter. The estimation of K comes from minimizing the square difference of experimental R_t^{obs} and SDFM R_t^{obs}. In some cases, the minimum value came from K=0. Due to that value having physically no sense, a value of close to 0 was entered instead. Depending on the proximity of K to 0, permeabilities boosted to values of more than 100 $\mu m/s$. For the analysis of these values, it is not important the exact amount (because it comes from an arbitrary value close to 0) but rather the fact that they are greater than those of the dominant salt and, therefore, less rejected than the ions of the dominant salt.

Table 10. Ion permeabilities $[\mu m/s]$

Species	NF270	NF90	DL
$\boldsymbol{Na^+}$	16,57	0,68	22,29
$\boldsymbol{Cl^-}$	17,25	1,61	22,29
NH_4^+	97,45	60,34	5,39
K^+	241,53	229,30	26,49
Mg^{2+}	6,83	0,28	1,68
Ca^{2+}	9,29	0,11	2,43
Br^-	10,92	0,07	13,62
NO_3^-	24,40	1,91	407,49
SO_4^{2-}	0,54	0,06	0,35
HCO_3^-	4,43	0,16	49,53
B^{3+}	3,89	2,29	39,34
Al^{3+}	0,10	6,51	8,19

Mn^{2+}	5,35	1,37	2,26
Ni^{2+}	0,52	0,02	4,44
Cu^{2+}	0,04	0,22	3,41
As^{3+}	0,53	8,28	0,58
Pb^{2+}	1,13	4,67	309,58

The highest permeabilities regarding the NF270 are for potassium (241,53 $\mu m/s$), nitrate (24,40 $\mu m/s$), bromide (10,92 $\mu m/s$) and ammonium (97,45 $\mu m/s$), which were the ions less rejected by the membrane. After those, the ions of the dominant salt had the biggest permeabilities (16,57 and 17,25 $\mu m/s$ for sodium and chloride, respectively). Afterwards, with the lowest permeabilities, are the divalent and trivalent ions, which were the best rejected, all according to the phenomenon of dielectric exclusion.

Similar to the NF270, the NF90 has ammonium and potassium as the highest ion permeabilities (60,34 and 229,30 $\mu m/s$ respectively). The permeabilities of the ions of the dominant salt were significantly lower than the ones obtained from the NF270. Concerning the rest of the trace ions, all had fairly low permeabilities but arsenic, lead and aluminium, which match the results of trace rejection stated in 5.4.2.

Finally, turning to the DL, average higher permeabilities compared to the other two membranes can be observed. Moreover, spikes in lead (309,58 $\mu m/s$), boron (39,34 $\mu m/s$), bicarbonate (49,53 $\mu m/s$) and nitrate (407,49 $\mu m/s$) permeabilities are stated. The permeabilities of the ions of the dominant salt (22,29 $\mu m/s$ for both sodium and chloride) were higher than both prior membranes. However, permeabilities of bromide and potassium were expected to be higher in order to match its rejection values (5.4.3).

5.6. Water quality achieved

In order to determine the quality of the filtrated water, the species that surpassed the recommended limits for Spanish drinking water guidelines (RD 140/2003) are displayed in Table 11. Those species are chloride, manganese and arsenic. The values shown at the permeate column are the resulting compositions after the nanofiltration process at 32 bar TMP. Iron compositions were not displayed due to being virtually nil, even though they were a key factor in the study of Jurado et. al (1). Ammonium

was also a key factor at the prior study. However the concentrations analysed at this projected resulted lower than stipulated in RD 140/2003, and thus, also not displayed. Feed solution used for each filtration experiment, while coming from the same source, experienced some variation in its concentration.

Table 11. Feed and permeate concentrations for NF270, NF90 and DL

Chemical parameter	NF270 Feed	NF270 Permeate	NF90 Feed	NF90 Permeate	DL Feed	DL Permeate	RD 140/2003
Chloride (ppm)	330	123	314,0	13,5	362,6	162,3	250,0
Manganese (ppb)	189,1	20,2	115,9	0,96	119,6	12,72	50,0
Arsenic (ppb)	26,5	0,35	23,8	3,74	328,7	41,56	10,0

The NF270 and NF90 reduced the concentration of all three species below the limit guidelines.

The DL reduced the concentration of chloride and manganese below the limit guidelines. Regarding to arsenic, there is a spike in the feed concentration way over the feed concentration of both membranes NF270 and NF90. Even having a slightly higher arsenic rejection than NF90, the DL did not achieve a permeate water with arsenic concentration below the drinkable limit.

Regarding chloride and manganese all membranes rejected the ions well below the drinkable limits. As far as arsenic is concerned, NF 270 rejected 99% being the one with the best rejection compared to the other two membranes, NF90 and DL, as for them the answer is not as clear; DL permeate did not achieve the status of drinkable water due to being 4 times over the limit. However the arsenic rejection of DL was similar than that of NF90 and still the permeate of NF90 did not surpass the limit. The only different variable here is the feed concentration. If the rejection curve of the DL stayed constant and with the same amount of arsenic in the feed concentration as the NF270 and NF90, its permeate flow would have stayed below the drinkable limits. This fact reflects the reality of water treatment that the sector faces; water compositions are not always constant and what can be used as a working solution today it might not work tomorrow.

Fixing the TMP at 32 bar, the permeate flux values for NF270, NF90 and DL are: 72,8; 46,9 and 42,5 µm/s, respectively; having a higher permeat flux allows the filtration system to treat more water. At

the same TMP, the arsenic rejections are, stated in the same order: 98%, 82% and 83%. This indicates that the best membrane to be utilised with the Besòs water is the NF270 due to its higher permeate flux and better arsenic rejection.

6. Environmental impact

The objective of this section is to analyse the environmental effects, both positive and negative, of the usage of the lab scale NF plant utilized in this project. The extension of the analysis will only include the impacts produced in the operation phase and not those from the construction phase of the plant.

First of all, it is necessary to identify the different aspects that play a role in environmental matters. These are defined as elements of the activities, products or services of an organization that can interact with the environment. Regarding this project, the environmental aspects are the following (45):

- Emissions: gaseous substances, dust, particles, fog, fumes, vapours, etc.
- Discharges: in the course of rivers, coasts or municipal collectors systems.
- Waste: urban, dangerous and inert.
- Acoustic pollution: noise and vibration.
- Consumption of resources: water, electricity and fuels.

Next and for the sake of simplicity in Table 12 the environmental aspects caused by the realization of this project are summarized. It shows the environmental factors in rows and the different environments in columns. Due to the nature of this project two more aspects will be added. Those are the intrinsic generation of products and by-products of a NF facility. A colour code is used that points out the positive effects (green), the negative effects (red), the negative effects caused by accidents or malfunctions (yellow) and neutral effects (white).

Table 12. Project environmental impact (46)

Lab scale plant	Abiotic medium			Biotic medium	Socio-economic and cultural factors		
	Air	**Water**	**Ground**	**Flora and fauna**	**Culture**	**Infrastructure**	**Economy and population**
Emissions and discharges							
Acoustic pollution and vibrations							
Energy consumption							
Product generation							
By-product generation							
Smell generation							

Regarding the abiotic medium the negative sources of contamination are the acoustic pollution generated by the pump (Figure 35) and the by-product generation that includes the concentrate from the NF process and residual chemicals that, if not treated correctly, may pose a threat to the environment. The by-product generation would also influence negatively in the biotic medium.

Turning to the socio-economic and cultural factors, there are three aspects that need to be taken into account. The first one is the consumption of energy that implies the operation of this plant that, while it's not as big as a RO plant, is still not insignificant.

The positive aspect of this project is the generation of higher quality water.

As far as accidents, missuses or equipment failure is concerned there would be jeopardy of water contamination, damaged infrastructure (in the case of, for example, the explosion of the pump), economic loses and personal injuries.

Figure 35. Pump used for the experiments without noise cancelling cover a), and with cover b); lateral view of the cover showing the layer of noise dampening foam.

7. Conclusions

In this project an assessment of the underground water quality of the Besòs area was carried out, as well as an analysis of the rejections of three NF membranes (NF270, NF90 and DL). Six experiments in total were carried out (two per each membrane) in a closed nanofiltration circuit using the Besòs water as feed solution. With the resulting permeate, laboratory analysis were conducted in order to determine its composition and therefore its quality.

For the water to be drinkable (according to the Spanish regulations), prior studies to this project were made and showed an excess of ammonium, manganese, arsenic and iron in the water. This project analysis of the water determined that the ion concentrations surpassing the drinkable limits were those of chloride, manganese and ammonium. These differences can be explained with: the dependence of the underground waters to seasonal changes, composition variations of the underground water inflows and chemical degradation during the experimentation phase.

The membrane NF270 rejected, at maximum TMP (32 bar), more than 85% of all the heavy metals. Moreover it achieved, under the same conditions, rejections of more than 80 % for all divalent ions and bicarbonate. Rejections of monovalent ions were fairly lower. Chloride, manganese and arsenic were successfully removed to values below the drinkable limits (123,0 ppm; 20,2 ppb and 0,35 ppb, respectively). Rejection of arsenic reached values of more than 98%. Under similar feed solutions than those treated in this project, filtration processes using NF270 are a valid option to produce drinkable water.

The membrane NF90 achieved higher global rejections than NF270 and DL. At maximum TMP, all divalent ions were rejected and even monovalent ions such as bromide and bicarbonate at more than 98%. Applying the same TMP, all heavy metals but two were rejected at more than 95%, being those two arsenic and lead. Lead presence does not pose a threat here, however arsenic does. Arsenic rejections reached a maximum of 81%. That is enough to make the water drinkable for feed concentrations lower than 52 ppb. However, with the variability of the Besòs underground water composition, it cannot be assured that this membrane would always be able to make its water drinkable. Further studies are need regarding NF90 membrane and water with high arsenic compositions in order to draw a final conclusion.

The membrane DL, although with similar behaviour than the NF270, achieved lower global rejections than the other two membranes. Similar to the other NF membranes, the rejection of divalent and trivalent ions was higher than monovalent ones. Working at maximum TMP, rejections of up to 90% for divalent ions were achieved. Monovalent ion rejection ranged from 40% to 70%. Regarding heavy metals, it achieved rejections lower than the other two membranes, except for arsenic, where it

achieved rejections similar to those of NF90 and even slightly higher. As far as arsenic is concerned, the same conclusion should be applied as with NF90.

As expected, the permeate flux and the TMP were linearly dependent. The membrane NF270 achieved the highest permeate flux when compared with the other membranes across the whole TMP domain. The SDFM was well-fitted as it produced accurate outcomes for the prediction of experimental rejection values.

The difference in rejection and permeate flux values between membranes comes from their structure. Even though all membranes are polyamide thin-film composite, each of them presents differences in the configurations of their functional groups. These variations allow for different manifestations of dielectric and Donnan exclusion phenomena that increase or decrease the flow of permeate and the ion permeability.

Budget

This section looks into the expenses incurred by the realization of this project.

- **Water expenses**

Distilled water was used to pressurize the membrane and to clean the hydraulic system before and after the experiment and also to clean the used lab material. Milli-Q water was used to prepare solutions and samples for chromatography, ICP and titration. These expenses are summarized in Table 13.

Table 13. Water use costs

Water	Amount (L)	Price (€/L)	Cost (€)
Distilled	610	0,32	195,2
Milli-Q	18	0,55	9,9
Total			205,1

- **Electricity expenses**

The main use of electricity was to power up the pump which was used for 48h with a power of 2,54 kW (47); resulting 121,92 kWh. The price of energy is set according to Endesa ratings of energy December of 2019 (Table 14).

The illumination of installations was not taken into account.

Table 14. Electricity use costs

Concept	Amount (kWh)	Price (€/kWh)	Cost (€)
Pump usage	121,92	0,1198	14,60
Total			14,60

- **Chemicals expenses**

The chemicals listed in Table 15 were used to obtain standards for the chromatography and ICP analysis

Table 15. Chemical use costs

Concept	Amount (g)	Price (€/kg)	Cost (€)
KCl	0,5	25,4	0,01
CaCl	0,5	17,1	0,01
NaF	0,5	30,9	0,02
KBr	0,5	85,8	0,04
$(NH_4)SO_4$	1,8	22,8	0,04
NaCl	0,5	15,7	0,01
KNO_3	0,5	27,8	0,01
MgCl	0,5	28,2	0,01
Na_3PO_4	0,5	32,9	0,02
NaHCO3	0,4	37,0	0,01
$Na_2(CO_3)$	0,4	18,5	0,01
HNO_3	0,2 (mL)	31 (€/L)	0,01
Total			0,20

- **Membrane material expenses**

A total of six membranes were used (three of each kind) and two spacers (Table 16).

Table 16. Membrane costs

Concept	Units	Price (€/unit)	Cost (€)
NF270 membrane	2	13,2	26,4
NF90 membrane	2	13,2	26,4
NF270 membrane	2	10,4	20,8
Spacers	2	15	30
Total			103,6

- **NF plant expenses**

The amortized costs of the pieces that form the NF plant are shown in Table 17. In order to calculate those costs the Eq. 10 is needed. The time of usage has been of 4 months, equivalent to the duration of this project.

$$Amortized\ cost = \frac{Equipment\ cost}{Useful\ life} \cdot\ time\ of\ usage \qquad \text{Eq. 10}$$

Table 17. Plant expenses

Equipment	Units	Price (€/unit)	Useful life (years)	Cost (€)
Pump G10 Hidra-Cell	1	3616	10	121
30L tank	1	50	5	3
Cooling system	1	2100	5	140
Flow meter	1	386	10	13
Needle valve	1	65	5	4

Tap valve	1	135	5	9
Variable frequency drive	1	910	10	30
PVC piping system	1	120	5	8
Membrane module	1	2200	10	73
Manual pump	1	420	10	14
Pre-cartridge filter	1	62	6	3
Capillary tube	1	15	10	1
Computer	1	400	5	27
Total				446

- **Laboratory equipment expenses**

Using also Eq. 10 the costs of the lab equipment usage have been calculated and are summarized in Table 18.

Table 18. Laboratory equipment expenses

Concept	Units	Price (€/unit)	Useful life (years)	Cost (€)
pH-meter	1	340	10	11
Conductivity meter	1	200	10	7
Precision scale	1	135	10	5
Ion chromatography system	1	11.900	10	397
Titrator	1	6.200	10	207

ICP	1	10.500	10	350
Total				977

- **Staff expenses**

Here are shown the costs of hiring personal for the realization of this project. According to "el Boletín Oficial del Estado" (BOE) the minimum salary of a recently graduated chemical engineer is 17.807 € per annum (48). Using as reference a worker that works 49 weeks a year, 40 hours a week, the salary is 9,1 €/hour. The costs broken down appear in Table 19. The salary for the directors of this project and the laboratory technician is set at, arbitrarily, 16€/hour.

Table 19. Salary costs

Concept	Units (hours)	Price (€/hours)	Cost (€)
Bibliographic research	100	9,1	910
Project writing	200	9,1	1820
Laboratory and experimental	440	9,1	4004
ICP analysis	10	16	160
Project review by directors	20	16	320
Total			7214

- **Total expenses**

The entire cost of the project is described in Table 20 being a total of: 8.960,5 €

Table 20. Total expenses

Concept	Cost (€)
Water	205,1
Electricity	14,6
Chemicals	0,2
Membrane material	103,6
NF plant expenses	446,0
Laboratory equipment	977,0
Staff expenses	7214,0
TOTAL	**8.960,5 €**

Bibliography

1. Jurado, A., Vázquez-Suñé, E. i Pujades, E. Potential uses of pumped urban groundwater: a case study in Sant Adrià del Besòs (Spain). A: *Hydrogeology Journal*. 2017, Vol. 25, núm. 6, p. 1745-1758. ISSN 14350157. DOI 10.1007/s10040-017-1575-3.

2. Malaeb, L. i Ayoub, G.M. Reverse osmosis technology for water treatment: State of the art review. A: *Desalination* [en línia]. 2011, Vol. 267, núm. 1, p. 1-8. ISSN 00119164. DOI 10.1016/j.desal.2010.09.001. Disponible a: http://dx.doi.org/10.1016/j.desal.2010.09.001.

3. Pages, N., Yaroshchuk, A., Gibert, O., Cortina, J.L. Rejection of trace ionic solutes in nanofiltration: Influence of aqueous phase composition. A: *Chemical Engineering Science*. 2013, Vol. 104, p. 1107-1115. ISSN 00092509. DOI 10.1016/j.ces.2013.09.042.

4. (WHO), W.H.O. Manganese in drinking-water: Background document for development of WHO Guidelines for Drinking-water Quality. A: *Geneva: WHO* [en línia]. 2011, Disponible a: https://apps.who.int/iris/bitstream/handle/10665/75376/WHO_SDE_WSH_03.04_104_eng.pdf.

5. De Munari, A. i Schäfer, A.I. Impact of speciation on removal of manganese and organic matter by nanofiltration. A: *Journal of Water Supply: Research and Technology - AQUA*. 2010, Vol. 59, núm. 2-3, p. 152-163. ISSN 00037214. DOI 10.2166/aqua.2010.067.

6. Cotton, A., Wikinson, G. *Química Inorgánica Avanzada*. 1973.

7. Ates, A. i Akgül, G. Modification of natural zeolite with NaOH for removal of manganese in drinking water. A: *Powder Technology* [en línia]. 2016, Vol. 287, p. 285-291. ISSN 1873328X. DOI 10.1016/j.powtec.2015.10.021. Disponible a: http://dx.doi.org/10.1016/j.powtec.2015.10.021.

8. Ityel, D. Ground water: Dealing with iron contamination. A: *Filtration and Separation* [en línia]. 2011, Vol. 48, núm. 1, p. 26-28. ISSN 00151882. DOI 10.1016/S0015-1882(11)70043-X. Disponible a: http://dx.doi.org/10.1016/S0015-1882(11)70043-X.

9. Hove, M., Van Hille, R.P. i Lewis, A.E. Mechanisms of formation of iron precipitates from ferrous solutions at high and low pH. A: *Chemical Engineering Science*. 2008, Vol. 63, núm. 6, p. 1626-1635. ISSN 00092509. DOI 10.1016/j.ces.2007.11.016.

10. Pang, F.M., Kumar, P., Teng, T.T., Mohd Omar, A.K., Wasewar, K. Removal of lead, zinc and iron by coagulation-flocculation. A: *Journal of the Taiwan Institute of Chemical Engineers* [en línia]. Taiwan Institute of Chemical Engineers, 2011, Vol. 42, núm. 5, p. 809-815. ISSN 18761070. DOI 10.1016/j.jtice.2011.01.009. Disponible a: http://dx.doi.org/10.1016/j.jtice.2011.01.009.

11. Li, M., Zhu, X., Zhu, F., Ren, G., Cao, G., Song, L. Application of modified zeolite for ammonium removal from drinking water. A: *Desalination* [en línia]. 2011, Vol. 271, núm. 1-3, p. 295-300. ISSN 00119164. DOI 10.1016/j.desal.2010.12.047. Disponible a: http://dx.doi.org/10.1016/j.desal.2010.12.047.

12. Malovanyy, A., Sakalova, H., Yatchyshyn, Y., Plaza, E., Malovanyy, M. Concentration of ammonium

from municipal wastewater using ion exchange process. A: *Desalination* [en línia]. 2013, Vol. 329, p. 93-102. ISSN 00119164. DOI 10.1016/j.desal.2013.09.009. Disponible a: http://dx.doi.org/10.1016/j.desal.2013.09.009.

13. Mondal, P., Majumder, C.B. i Mohanty, B. Laboratory based approaches for arsenic remediation from contaminated water: Recent developments. A: *Journal of Hazardous Materials*. 2006, Vol. 137, núm. 1, p. 464-479. ISSN 03043894. DOI 10.1016/j.jhazmat.2006.02.023.

14. Jiang, J.Q. Removing arsenic from groundwater for the developing world - A review. A: *Water Science and Technology*. 2001, Vol. 44, núm. 6, p. 89-98. ISSN 02731223. DOI 10.2166/wst.2001.0348.

15. Garelick, H., Dybowska, A., Valsami-Jones, E., Priest, N. Remediation technologies for arsenic contaminated drinking waters. A: *Journal of Soils and Sediments*. 2005, Vol. 5, núm. 3, p. 182-190. ISSN 14390108. DOI 10.1065/jss2005.06.140.

16. Kim, J. i Benjamin, M.M. Modeling a novel ion exchange process for arsenic and nitrate removal. A: *Water Research*. 2004, Vol. 38, núm. 8, p. 2053-2062. ISSN 00431354. DOI 10.1016/j.watres.2004.01.012.

17. Wang, L. K., Chen, J. P., Hung, Y. T., & Shammas, N.K. *Membrane and desalination technologies (Vol. 13)*. 2008.

18. Richard W. Baker. *Membrane Technology and Applications, Second Edition* [en línia]. 2004. ISBN 0470854456. Disponible a: http://onlinelibrary.wiley.com/book/10.1002/0470020393.

19. Comparison Membrane Techniques. A: [en línia]. [Consulta: 11 novembre 2019]. Disponible a: https://www.logisticon.com/en/technologies/membrane-filtration.

20. Mohammad, A.W., Teow, Y. H., Ang, W. L., Chung, Y. T., Oatley-Radcliffe, D. L., Hilal, N. Nanofiltration membranes review: Recent advances and future prospects. A: *Desalination* [en línia]. 2015, Vol. 356, p. 226-254. ISSN 00119164. DOI 10.1016/j.desal.2014.10.043. Disponible a: http://dx.doi.org/10.1016/j.desal.2014.10.043.

21. Reig, M., Pagès, N., Licon, E., Valderrama, C., Gibert, O., Yaroshchuk, A., Cortina, J.L. Evolution of electrolyte mixtures rejection behaviour using nanofiltration membranes under spiral wound and flat-sheet configurations. A: *Desalination and Water Treatment*. 2015, Vol. 56, núm. 13, p. 3519-3529. ISSN 19443986. DOI 10.1080/19443994.2014.974215.

22. Million Insights: Cross Flow Membrane Market – Growth, Future Prospects and Competitive Analysis by 2021. A: [en línia]. [Consulta: 10 desembre 2019]. Disponible a: https://millioninsights.blogspot.com/2018/04/cross-flow-membrane-market.html.

23. AMTA. Reverse Osmosis Membrane Separation. A: [en línia]. [Consulta: 11 gener 2020]. Disponible a: https://www.amtaorg.com/Reverse_Osmosis_Membrane_Separation.html.

24. Ribera, G., Llenas, L., Martínez, X., Rovira, M., de Pablo, J. Comparison of nanofiltration membranes' performance in flat sheet and spiral wound configurations: a scale-up study. A: *Desalination and Water Treatment* [en línia]. 2013, Vol. 51, núm. 1-3, p. 458-468. ISSN 1944-3994. DOI 10.1080/19443994.2012.714527. Disponible a: https://doi.org/10.1080/19443994.2012.714527.

25. Mulder, M. *Basic principles of membrane technology.* 2012.

26. Peeters, J.M.M., Mulder, M.H.V. i Strathmann, H. Streaming potential measurements as a characterization method for nanofiltration membranes. A: *Colloids and Surfaces A: Physicochemical and Engineering Aspects*. 1999, Vol. 150, núm. 1-3, p. 247-259. ISSN 09277757. DOI 10.1016/S0927-7757(98)00828-0.

27. Uribe, B.E.C., Miranda, D.M.I.A. i Costa, D.E.S. Estudio del proceso de nanofiltración para la desminerlización de lactosuero dulce . A: *Departamento de ingeniería química y nuclear* [en línia]. 2005, Vol. Doctor, p. 322. DOI 10.4995/Thesis/10251/1878. Disponible a: https://riunet.upv.es/bitstream/handle/10251/1878/tesisUPV2361.pdf.

28. Bandini, S. i Vezzani, D. Nanofiltration modeling: The role of dielectric exclusion in membrane characterization. A: *Chemical Engineering Science*. 2003, Vol. 58, núm. 15, p. 3303-3326. ISSN 00092509. DOI 10.1016/S0009-2509(03)00212-4.

29. Schoch, R.B., Han, J. i Renaud, P. Transport phenomena in nanofluidics. A: *Reviews of Modern Physics*. 2008, Vol. 80, núm. 3, p. 839-883. ISSN 00346861. DOI 10.1103/RevModPhys.80.839.

30. Bhattacharjee, S., Chen, J.C. i Elimelech, M. Coupled model of concentration polarization and pore transport in crossflow nanofiltration. A: *AIChE Journal*. 2001, Vol. 47, núm. 12, p. 2733-2745. ISSN 00011541. DOI 10.1002/aic.690471213.

31. Al-Rashdi, B.A.M., Johnson, D.J. i Hilal, N. Removal of heavy metal ions by nanofiltration. A: *Desalination*. 2013, Vol. 315, p. 2-17. ISSN 00119164. DOI 10.1016/j.desal.2012.05.022.

32. Häyrynen, K., Pongrácz, E., Väisänen, V., Pap, N., Mänttäri, M., Langwaldt, J., Keiski, R.L. Concentration of ammonium and nitrate from mine water by reverse osmosis and nanofiltration. A: *Desalination*. 2009, Vol. 240, núm. 1-3, p. 280-289. ISSN 00119164. DOI 10.1016/j.desal.2008.02.027.

33. Potgieter, J.H., McCrindle, R. I., Sihlali, Z., Schwarzer, R., Basson, N. Removal of iron and manganese from water with a high organic carbon loading. Part I: The effect of various coagulants. A: *Water, Air, and Soil Pollution*. 2005, Vol. 162, núm. 1-4, p. 49-59. ISSN 00496979. DOI 10.1007/s11270-005-5992-x.

34. Sato, Y., Kang, M., Kamei, T., Magara, Y. Performance of nanofiltration for arsenic removal. A: *Water Research*. 2002, Vol. 36, núm. 13, p. 3371-3377. ISSN 00431354. DOI 10.1016/S0043-1354(02)00037-4.

35. Yan, Z.Q., Zeng, L.M., Li, Q, Liu, T.Y., Matsuyama, H., Wang, X.L. Selective separation of chloride and sulfate by nanofiltration for high saline wastewater recycling. A: *Separation and Purification Technology* [en línia]. 2016, Vol. 166, p. 135-141. ISSN 18733794. DOI 10.1016/j.seppur.2016.04.009. Disponible a: http://dx.doi.org/10.1016/j.seppur.2016.04.009.

36. Sheet, P.D. Product Data Sheet FILMTEC ™ NF270-400 / 34i Element Description Ideal for : utility managers and operators dealing with surface and Product Type Typical Properties Element Dimensions Operating and Additional Important Information Product Stewardship Befo. A: . 2019, núm. 609, p. 3-5.

37. Ang, W. L., Mohammad, A. W., Benamor, A., Hilal, N. Hybrid coagulation-NF membrane processes

for brackish water treatment: Effect of pH and salt/calcium concentration. A: *Desalination* [en línia]. 2016, Vol. 390, p. 25-32. ISSN 00119164. DOI 10.1016/j.desal.2016.03.018. Disponible a: http://dx.doi.org/10.1016/j.desal.2016.03.018.

38. Diop, S. N., Diallo, M. A., Diawara, C. K., Cot, D. Intrinsic properties and performances of NF270 and XLE membranes for water filtration. A: *Water Science and Technology: Water Supply*. 2011, Vol. 11, núm. 2, p. 186-193. ISSN 16069749. DOI 10.2166/ws.2011.024.

39. Membranes, F.N.-. Data sheet: FilmTec™ NF90-400/34i. A: [en línia]. p. 1-2. Disponible a: https://www.dupont.com/products/filmtecnf9040034i.html.

40. Idil Mouhoumed, E., Szymczyk, A., Schäfer, A., Paugam, L., La, Y. H. Physico-chemical characterization of polyamide NF/RO membranes: Insight from streaming current measurements. A: *Journal of Membrane Science*. 2014, Vol. 461, p. 130-138. ISSN 18733123. DOI 10.1016/j.memsci.2014.03.025.

41. DOW NF90 Nanofiltration (NF) Membrane, 47 mm Size - YMNF90475 | S. A: [en línia]. [Consulta: 15 gener 2020]. Disponible a: https://www.sterlitech.com/nanofiltration-nf-membrane-ymnf90475.html.

42. Lopez, J., Reig, M., Vecino, X., Valderrama, C., Gibert, O., Torres, E. Evaluation of polymeric nanofiltration membranes on metal valorisation from acidic mine waters. A: *Special Edition for Euromembrane 2018 Conference*. p. 1254-1255.

43. Base, W. i Macroporous, A. Data sheet: DL series GE POWER. A: . 2007, Vol. 13, p. 261.

44. Vecino, X., Reig, M., Bhushan, B., Gibert, O., Valderrama, C., Cortina, J. L. Liquid fertilizer production by ammonia recovery from treated ammonia-rich regenerated streams using liquid-liquid membrane contactors. A: *Chemical Engineering Journal*. Elsevier, 2019, Vol. 360, núm. December 2018, p. 890-899. ISSN 13858947. DOI 10.1016/j.cej.2018.12.004.

45. Peña, A.C. Aspectos ambientales: identificación y evaluación. AENOR (Asociación Española de Normalización y Certificación). A: . 2007,

46. Rafael, R. TFG: Eliminació de metalls mitjançant membranes de nanofiltració: Efecte de la concentració d'alumini i ferro. A: *ETSEIB, UPC Barcelona*. 2007,

47. Flow, M. Data sheet: G10 Series Maximum Flow Rate. A: [en línia]. Disponible a: https://www.hydra-cell.co.uk/Pump-Selection/Metric/1830-/G10.

48. Trabajo, M.D.E. i Social, Y.S. Boletín Oficial del Estado: Ministerio De Trabajo , Migraciones. A: . 2019, p. 32526-32554.